Science of the Total Environment 812 (2022) 152412

Contents lists available at ScienceDirect

Science of the Total Environment

journal homepage: www.elsevier.com/locate/scitotenv

Evidence of Covid-19 lockdown effects on riverine dissolved organic matter dynamics provides a proof-of-concept for needed regulations of anthropogenic emissions

S. Retelletti Brogi [a,*], G. Cossarini [b], G. Bachi [a], C. Balestra [b], E. Camatti [a,c], R. Casotti [d], G. Checcucci [a], S. Colella [e], V. Evangelista [a], F. Falcini [e], F. Francocci [f], T. Giorgino [g], F. Margiotta [d], M. Ribera d'Alcalà [d,f], M. Sprovieri [h], S. Vestri [a], C. Santinelli [a,*]

[a] Istituto di Biofisica, CNR, Pisa, Italy
[b] Istituto Nazionale di Oceanografia e Geofisica Sperimentale. Sgonico (TS), Italy
[c] Istituto di Scienze Marine, CNR, Venezia, Italy
[d] Stazione Zoologica Anton Dohrn, Napoli, Italy
[e] Istituto di Scienze Marine, CNR, Roma, Italy
[f] Istituto per lo studio degli impatti Antropici e Sostenibilità in ambiente marino, CNR, Roma, Italy
[g] Istituto di Biofisica, CNR. Milano, Italy
[h] Istituto per lo studio degli impatti Antropici e Sostenibilità in ambiente marino, CNR. Campobello di Mazara (TP), Italy

HIGHLIGHTS

- Covid-19 lockdown affected riverine DOM dynamics.
- 44% less DOC in the river due to anthropic activities stopped during the lockdown.
- Small river quickly respond to the relief of anthropogenic pressure.
- Changed DOM dynamics affected the microbial loop in the river.
- Regulations of anthropogenic emission could improve riverine water quality.

GRAPHICAL ABSTRACT

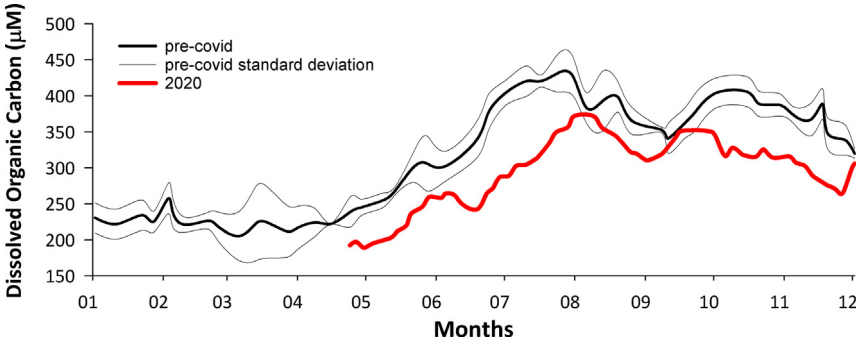

ARTICLE INFO

Article history:
Received 5 October 2021
Received in revised form 9 December 2021
Accepted 10 December 2021
Available online 16 December 2021

Editor: Ouyang Wei

ABSTRACT

The fast spread of SARS-CoV-2 virus in Italy resulted in a 3-months lockdown of the entire country. During this period, the effect of the relieved anthropogenic activities on the environment was plainly clear all over the country. Herein, we provide the first evidence of the lockdown effects on riverine dissolved organic matter (DOM) dynamics. The strong reduction in anthropogenic activities resulted in a marked decrease in dissolved organic carbon (DOC) concentration in the Arno River (−44%) and the coastal area affected by its input (−15%), compared to previous conditions. The DOM optical properties (absorption and fluorescence) showed a change in its quality, with a shift toward smaller and less aromatic molecules during the lockdown. The reduced human activity and the consequent change in DOM dynamics affected the abundance and annual dynamics of heterotrophic prokaryotes. The results of this study

* Corresponding authors.
E-mail addresses: simona.retelletti@ibf.cnr.it (S. Retelletti Brogi), gcossarini@inogs.it (G. Cossarini), cbalestra@inogs.it (C. Balestra), elisa.camatti@ismar.cnr.it (E. Camatti), raffa@szn.it (R. Casotti), giovanni.checcucci@ibf.cnr.it (G. Checcucci), simone.colella@cnr.it (S. Colella), valtere.evangelista@ibf.cnr.it (V. Evangelista), federico.falcini@cnr.it (F. Falcini), fedra.francocci@cnr.it (F. Francocci), toni.giorgino@cnr.it (T. Giorgino), margiot@szn.it (F. Margiotta), maurizio@szn.it (M. Ribera d'Alcalà), Mario.sprovieri@cnr.it (M. Sprovieri), stefano.vestri@ibf.cnr.it (S. Vestri), chiara.santinelli@ibf.cnr.it (C. Santinelli).

http://dx.doi.org/10.1016/j.scitotenv.2021.152412

Keywords:
Lockdown
DOM
Carbon cycle
Riverine inputs
Arno River

highlight the extent to which DOM dynamics in small rivers is affected by secondary and tertiary human activities as well as the quite short time scales to return to the impacted conditions. Our work also supports the importance of long-term research to disentangle the effects of casual events from the natural variability.

1. Introduction

Rivers connect a large portion of Earth's land surface to the ocean; their input of a large amount of organic matter and nutrients stimulates biological activity in coastal areas, contributing to making them one of the most productive ecosystems on the Earth. Riverine inputs therefore have a profound impact on the biogeochemistry of the world's oceans, playing a crucial role in the global biogeochemical cycles (Aufdenkampe et al., 2011). Because of its importance, riverine water quality is monitored worldwide, and several parameters (e.g. oxygen, inorganic nutrients, pH, bacterial load, heavy metals, contaminants) are measured in order to evaluate the ecosystem status. Monitoring programs do not take into account dissolved organic matter (DOM), even if it has been demonstrated that human-related activities have induced changes in the quantity and quality of DOM in rivers (Stanley et al., 2012; Xenopoulos et al., 2021). Through the years, anthropogenic activities have increased the input of DOM to the aquatic environment, and since anthropogenic DOM is different from the natural one, being either more recalcitrant (e.g. the black carbon produced by combustion), or more labile (e.g. DOM from wastewaters or urban sewage) (Xenopoulos et al., 2021), it can impact the functioning of riverine ecosystems and the CO_2 fluxes from the rivers to the atmosphere. Being the main source of energy for heterotrophic prokaryotes, DOM fuels the microbial loop (Carlson and Hansell, 2015), whose proper functioning regulates the dynamics of the whole food web, channeling energy toward the higher trophic levels (Williams et al., 2019). DOM also screens aquatic organisms from harmful UV radiation (Stedmon and Nelson, 2015) and directly influences the bioavailability of pollutants (Aiken et al., 2011). Modification of DOM natural dynamics can therefore strongly affect the wellbeing of riverine ecosystems, and consequently of the coastal areas impacted by riverine inputs. For instance, an excess of DOM can limit the light available to primary producers (Thrane et al., 2014; Wikner and Andersson, 2012) or can be associated with eutrophication, leading to a shift toward a net heterotrophy of the ecosystem (Deininger and Frigstad, 2019; Wikner and Andersson, 2012). DOM concentration and dynamics in rivers is the result of the interplay among the inputs from natural (e.g. in-situ production, soil leaching of plant root exudates) and anthropic (e.g. industries, agriculture, oil combustion, water treatment plant) processes, and the physico-chemical and biological re-elaboration and removal of these inputs within the soil and the river itself. It can be therefore considered as a synthetic ecosystem descriptor and, as such, a very good proxy for aquatic ecosystems' health (Deininger and Frigstad, 2019).

But what happens if the anthropogenic pressure is relieved or significantly reduced? How will DOM dynamics respond in rivers and coastal areas? What timeframe is needed to observe a response? The lockdown due to the COVID-19 pandemic represented an unprecedented opportunity to answer these questions. In different parts of the world, the relief of anthropic activities due to the COVID-19 control policies had a strong impact on the quality of both air and surface waters. Indeed, the marked reduction of the monitored atmospheric pollutants (e.g. CO, CO_2, NO_x, SO_x, $PM_{2.5}$, PM_{10}, hydrocarbons, etc.) (Elsaid et al., 2021, and references therein) was observed. In over polluted rivers, an improvement of the Water Quality Indexes (Dutta et al., 2020; Patel et al., 2020), the decrease of heavy metal loads (Shukla et al., 2021), and the restoration of natural bacterial communities (Jani et al., 2021) were also reported. Since DOM dynamics is driven by the interaction of several factors, it shows a non-linear response to changes in environmental forcing and human pressure. As a consequence, DOM cannot be considered in the same way as a pollutant and a decrease in its concentration cannot be considered a necessary effect of the lockdown. Yet, taking into consideration the impact of human activities on riverine DOM, it is reasonable to hypothesize that the shut-down of a significant fraction of human activities would result in a change in DOM dynamics.

In this paper, we show the first evidences and quantification of the lockdown effects on riverine DOM dynamics in the Arno River (Tuscany, Italy). This river (average discharge 86 $m^3\ sec^{-1}$, drainage basin 8228 Km^2) is characterized by a torrential hydrological regime (Retelletti Brogi et al., 2020), high Dissolved Organic Carbon (DOC) concentration (Retelletti Brogi et al., 2015, 2020; Santinelli, 2015), a medium-high anthropogenic impact (Fig. 1), and it can be considered as a case study for DOM dynamics in small Mediterranean rivers with similar characteristics and human impact (Retelletti Brogi et al., 2020). The high-resolution record of DOM concentration and optical properties (absorption and fluorescence) available for 2014 and 2015, years with contrasting riverine discharge covering a wide spectrum of river variability (Retelletti Brogi et al., 2020), offers a unique chance to compare the data collected in the COVID era with the pre-lockdown regime.

2. Methods

2.1. Samples collection and treatment

In order to evaluate the effect of the lockdown on riverine DOM, samples were collected (1) from the spring to the mouth of the river; (2) in the lower part of the river, with a high temporal resolution; (3) in the coastal area in front of the river mouth.

(1) On March 5th, 2021, samples were collected at 14 stations along the river, upstream and downstream of the main tributaries, cities, and industrial areas (Fig. 1). This period was chosen since previous data showed the lowest DOM concentration in March, with a main terrestrial origin, coincident with the lowest autotrophic activity (Retelletti Brogi et al., 2020).
(2) From April 2020 to May 2021, surface river samples were collected two times a week in the lower part of the river in Pisa (station 14, Fig. 1), at the same location where samples were collected from January 2014 to December 2015 (Retelletti Brogi et al., 2020). A high temporal resolution sampling, whose importance is often underestimated, is necessary to be able to discriminate between the effect of a temporary relieve of anthropic pressure, such as the COVID-19 lockdown, and the effect of other disturbance events (e.g. floods or drought) that can have short-time effects (i.e. day or week).
(3) On May 5th 2020, 15 surface samples were collected within 12 miles from the coast and 7 miles northward and southward of the Arno River estuary.

All samples were collected into 2 l HCl-cleaned polycarbonate bottles (Nalgene), rinsed 3 times with the sample before filling, and kept refrigerated and in the dark until filtration, within a few hours from the sampling (1 h for the weekly samples). The samples were filtered by using a pre-washed 0.2 μm pore size Polycap filter (Whatman Polycap, 6705–3602 capsules) into HCl-cleaned 60 ml polycarbonate bottles (Nalgene), rinsed 3 times with the filtrate before filling, and measured immediately after filtration.

2.2. Analytical measurements

Dissolved organic carbon (DOC) concentration was measured to obtain quantitative information on DOM concentration. DOC was measured with

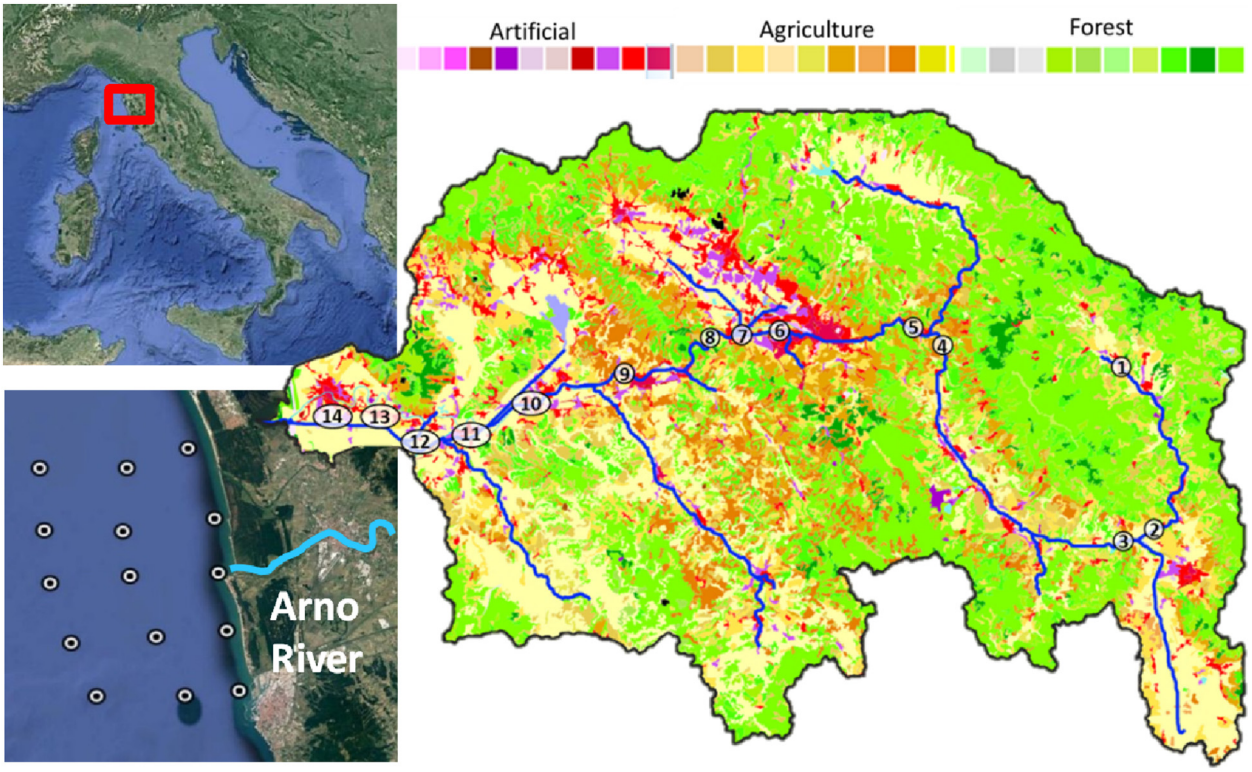

Fig. 1. Arno River basin's land coverage. Data from Copernicus Land Monitoring Service (CLC2018). The map is realized by using QGIS software (v. 3.12). The numbers refer to the location of the sampling stations along the river. The tributary between stations 2 and 3 is the Canale della Chiana; the tributary between stations 7 and 8 is the Ombrone Pistoiese; the tributary between stations 10 and 11 is the Usciana. The map on the left bottom corner shows the location of the coastal stations. (For interpretation of the references to colour in this figure legend, the reader is referred to the web version of this article.)

an analytical precision of ±1 μM by using a Shimadzu Total Organic Carbon analyzer (TOC-Vcsn), following the method described in Santinelli et al. (2015). DOC Reference Material (Hansell, 2005) was used to verify the instrument performance (CRM Batch #19 nominal concentration of 40–43 μM; measured concentration 41.5 ± 1.1 μM, $n = 81$).

Absorbance spectra were measured in a 10 cm quartz cuvette using a Jasco UV–visible spectrophotometer (Mod-7850) according to Retelletti Brogi et al. (2020). The absorption coefficient at 254 nm (a_{254}) and the spectral slope between 275 and 295 nm ($S_{275–295}$) were calculated by using the ASFit tool (Omanović et al., 2019). Since primary CDOM absorption is caused by conjugated systems present in organic compounds having the peak of absorption near 254 nm, a_{254} can be used to have quantitative information on CDOM (Del Vecchio and Blough, 2004). The $S_{275–295}$ was calculated to obtain information on the change in the DOM properties since its values are inversely related to the average molecular weight and aromaticity of the molecules.

Fluorescence excitation-emission Matrixes (EEMs) were obtained using the Aqualog spectrofluorometer (Horiba) according to Retelletti Brogi et al. (2020). The EEMs were elaborated using the TreatEEM software (Omanović Dario, TreatEEM—program for treatment of fluorescence excitation-emission matrices, https://sites.google.com/site/daromasoft/home/treateem). A blank EEM (Milli-Q water) was subtracted from each EEM and they were corrected for inner-filter effect (Lakowicz, 2006). The Rayleigh and Raman scatter peaks were removed by using a shape-preserving monotone cubic interpolation (Carlson and Fritsch, 1989). PARAFAC analysis (drEEM Toolbox, Murphy et al., 2013) was carried out on the EEMs, by merging the 2020–2021 dataset with the data from 2014 to 2015 (533 EEMs total). The validation of the PARAFAC model was performed by (i) analyzing the sum of squared error for different models (Fig. S1); (ii) visual inspection of the residuals between different models (Fig. S2); (iii) core consistency results (Fig. S3); (iv) split-half analysis results (Fig. S4); and (v) percentage of explained variance (99.6%, Fig. S5). The analysis resulted in the validation (Fig. S5) of a 6-component model (Fig. S6 and S7, Table S1). The emission and excitation spectra of the components (Fig. S6) were compared with those published by using the OpenFluor database (Murphy et al., 2014) and characterized as follows, component 1: microbial humic-like compounds ($C1_{mh}$); component 2: terrestrial humic-like compounds ($C2_{th}$); components 3 and 5: fulvic-like compounds ($C3_f$, $C5_f$); component 4: protein-like compounds ($C4_p$); component 6: polycyclic aromatic hydrocarbons ($C6_{pah}$) (see Table S1 for further information and Retelletti Brogi et al., 2020 for details on components identification). For each sample, the total fluorescence was calculated as the sum of the 6 components and normalized by the DOC concentration in order to evaluate the changes in fluorescence regardless of the variation in concentration.

One ml samples for Heterotrophic Prokaryotes (HP) Abundance (HPA) were fixed for 10 min with glutaraldehyde (GL, 0.05% final concentration) and stored at −80 °C until the analysis. After thawing, samples were stained with SYBR Green (Invitrogen Milan, Italy) 10^{-3} dilution of stock solution for 15 min at room temperature. Cell concentrations were assessed using a FACSVerse flow cytometer (BD BioSciences Inc., Frankyn Lakes, USA) equipped with a 488 nm Ar laser and a standard set of optical filters, at the Flow Cytometry Facility of the Stazione Zoologica Anton Dohrn of Naples, Italy. FCS Express software was used for analyzing the data and HP were discriminated from other particles based on scattering and green fluorescence from SYBR Green (Balestra et al., 2011).

2.3. Environmental conditions

Temperature and conductivity were measured with a portable multiparameter probe (Hanna HI98194). Daily average river discharge, precipitation, and air temperature were downloaded from the Regional Hydrological Service (www.sir.toscana.it). Precipitation data for 122 meteorological stations since 2004 were averaged in order to reconstruct the climatology.

2.4. Socio-economic data

Data and information on the anthropic activities within the Arno River basin affected by the lockdown were gathered from regional and national databases.

Industrial activity is expressed as an index of regional industrial production at the provincial-sectorial level in Tuscany (IRIP). The IRIP indicator is elaborated by the Regional Institute for economic planning of Tuscany (IRPET) and describes the evolution of industrial production within the Tuscany region. Data on the arrival of foreign tourists, as well as the movement of local people for tourism, were obtained from the statistics division of the Tuscany Region (https://www.regione.toscana.it/statistiche/dati-statistici/turismo); these data are publicly available on an annual basis. Data on transportation were gathered from, (i) the Italian Civil Aviation Authority (ENAC), which provides information about the airplane's movements (in or out) from each Italian airport on an annual basis, and (ii) the Google community mobility report, which provides the percentage of variation inland transportation, categorized according to the purpose of the movement, related to a baseline (calculated as the median value, for the corresponding day of the week, during the 5 weeks Jan 3–Feb 6, 2020; https://www.google.com/covid19/mobility/).

2.5. Statistical analyses

For all the parameters, the significance of the differences between the years (2014, 2015, 2020–2021) was tested by using the Kruskal–Wallis test (Origin software). Differences were considered significant at the threshold of $p < 0.05$. A principal component analysis (PCA, Legendre and Legendre, 2012) was applied to the data of the 6 FDOM components after standardization of the variables. PCA was performed using the R software (Team R Development Core, 2018). A stepwise regression approach (Draper and Harry, 1998) was used to analyze DOC temporal variability versus some explanatory variables that track sources and processes driving DOC evolution in the river. At each step of the regression analysis, independent variables were chosen if their contribution to the model was significant. Among the explanatory variables, the water temperature represents a proxy of the autochthonous DOC production, while bacteria abundance is a proxy for the potential decomposition rate of DOC. River discharge is used to describe the soil leaching and transport of DOC during flood events. Given that the flood duration can last from 1 to several days and the sampling could not catch the exact moment of the highest correlation value between DOC concentration and runoff (Retelletti Brogi et al., 2020), we tested the 1, 2 and 3 days discharge averages before the sampling. Additionally, since drought periods enhance the accumulation of organic matter in the soil that can be leached and transported by a flood event, we included in the model the discharge averages for the 30, 60, 90, 120 days before the sampling. Finally, we chose to add some dummy variables (i.e., variables assuming the values of 1 in a specific period and 0 otherwise) to indicate the presence (1) or absence (0) of the COVID-19 lockdown impacts on human activities (e.g., tourism, transport, industry, agriculture). Thus, we tested the hypothesis that allochthonous DOC production and transport into the river have been impacted by the reduction of human activities during the lockdown. Since the timing of the reduction of human activities during 2020 cannot be identified precisely (i.e., there have been possible mismatches between Italian restriction regulations and the effective reductions of human activities) we build several dummy variables and let the stepwise regression analysis select the most statistically relevant lockdown period. The analysis was performed with the stepwise fit Matlab statistical toolbox that uses an initial constant model and takes forward steps to include new variables based on their statistical significance (F-statistics at p-level or 0.025).

2.6. Remote sensing analysis

Weekly data from 2016 to 2019 were used to obtain the weekly climatology, which is then used as a reference for the analysis. The analysis of Chlorophyll-a (Chl-a) concentration was based on the Sentinel-3 OLCI (Ocean and Land Colour Instrument) full spatial resolution imagery, which properly captures the fine-scale variability associated with the coastal environment. We collected the full-time series (May 2016 – to present) of OLCI Level-2 full resolution (300 m) data from the EUMETSAT (European operational satellite agency for monitoring weather, climate and the environment from space) data center. Level-2 products were then extracted and remapped over a regular equirectangular grid off the Arno River mouth. We applied the CMEMS (Copernicus Marine Environment Monitoring Service) operational regional algorithms for phytoplankton chlorophyll retrieval (Volpe et al., 2019), adapted to OLCI bands, and implemented daily. The OLCI daily time series is then turned into a weekly time series by averaging on a pixel-by-pixel basis. For each pixel, the average and standard deviation are computed from a data cube of 3 pixels × 3 pixels × 7 days. This averaging reduces the impact of possible noise, common at these small scales, and increases spatial coverage mined by lack of data mostly due to clouds. The climatology has the same spatial resolution as the weekly data to which it is compared (nominally 300 m). Finally, we consider the difference between the 2020 weekly observations and the weekly climatology at the scale of the pixel, expressed as weekly mean anomalies (WMA):

$$WMA = \frac{Weekly_{Observations\,2020} - Weekly_{Climatology\,2016-2019}}{Weekly_{Climatology\,2016-2019}}$$

3. Results

3.1. Allochthonous sources of DOM to the Arno River

The samples, collected from the spring to the mouth of the river in March 2020 (sampling 1 in the methods), allowed for the identification of the main DOM enrichment areas within the river drainage basin and therefore for the primary allochthonous sources of DOM to the Arno River. A 125 μM DOC total enrichment was observed from the spring (50 μM) to the mouth of the river (175 μM) (Fig. 2), approximately 0.5 μM DOC per km. The increase is not linear and point source effects were observed along the river path. The highest increase in DOC (+ 130 μM) was observed downstream station 2 (after the Canale della Chiana tributary, Fig. 1) although the 43% of DOC enrichment was removed after the input of this tributary (Fig. 2) suggesting its labile form. Surprisingly, after Florence (station 6, Fig. 1), the biggest city along the river, a slight decrease in DOC

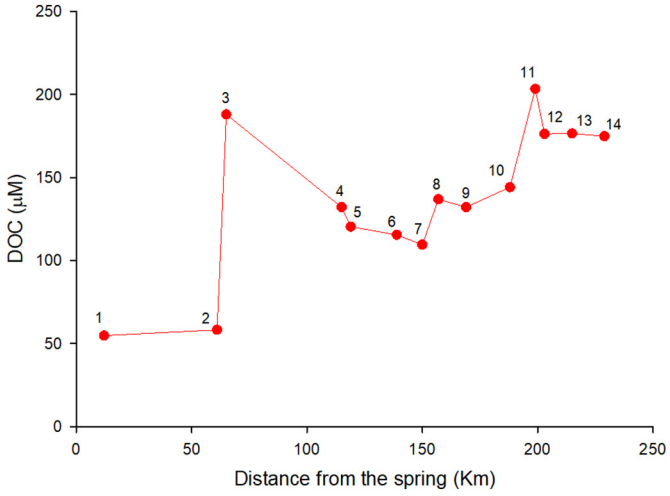

Fig. 2. DOC concentration from the spring to the mouth of the Arno River. The numbers refer to the sampling stations (their location on the basin is shown in Fig. 1).

was observed (Fig. 2). The Ombrone Pistoiese (discharging between stations 7 and 8, Fig. 1), and the Usciana (discharging between stations 10 and 11, Fig. 1) tributaries determined a 28 and 59 μM DOC enrichment, respectively (Fig. 2). Downstream station 12 no change in DOC was observed (Fig. 2). Specifically, the Canale della Chiana tributary (between stations 2 and 3, Fig. 1) drains an area mostly used as agricultural land, and passes through a gold processing industrial area; the Ombrone Pistoiese tributary (between stations 7 and 8, Fig. 1) drains a region that is characterized by a large portion of agricultural land, with a large number of greenhouses, and by the presence of textile industries; the Usciana tributary (between stations 10 and 11, Fig. 1) receives the wastewater from many tanneries and paper-mills. All these anthropic activities may represent an important source of DOM to the Arno River, although, due to the large spatial coverage of agriculture areas (Fig. 1), the main input is expected to come from the intensive agriculture activities. The unexpected lack of DOC enrichment after the city of Florence, and the many small cities located along the river, is due to the high biological lability of the DOM pool within the urban wastewaters (Regnier et al., 2013), allowing its rapid removal by the microbial community. This observation is further supported by the evidence of enhanced chemical oxygen demand measured after the Florence settlement (Cortecci et al., 2009).

3.2. How the lockdown affected the anthropogenic activities in Tuscany

Tuscany was one of the Italian regions most affected by the lockdown. During (March–May 2020) and immediately after (June 2020) the lockdown, the decrease in industrial production (−21.9%) was higher than the national one (−18.6%; IRPET, 2020). This depends on the industrial sectorial composition of Tuscany that is specialized in those sectors that more than all the others were affected by the lockdown restrictions.

A drastic reduction of all the industrial activities (−50%) was observed in April 2020, with values slowly going back to the pre-lockdown values since August 2020 (Fig. S8a). Compared to the average between 2012 and 2019, in 2020, a 57% reduction in the total tourist arrivals (−7.5 million people), 79% if considering only the foreign tourist, was registered in Tuscany (Fig. S8b). These data are available only on a yearly time scale, implying that these percentages would have been much more relevant if only the months of the lockdown would have been taken into account. The reduction of tourists, as well as the restrictions to travel, was also reflected in a 54% decrease in air traffic (i.e. 67,574 less airplane movements) in the two major airports in Tuscany (Pisa and Florence), compared to the average between 2014 and 2019 (Fig. S8c). A drastic reduction in inland transportation was also observed. The 2020 Google community mobility report shows a decrease of up to −97% between February and May 2020 (Fig. S8d).

Regarding the food compartment, the publicly available data from the Tuscany Region database suggest that in 2020 agriculture was not significantly affected by the lockdown restrictions. The total cultivated agricultural land was $9.63{\cdot}10^{16}$, $9.78{\cdot}10^{16}$, and $9.63{\cdot}10^{16}$ Ha in 2018, 2019, and 2020, respectively. Yet, it is not possible to exclude an effect on specific cultivation type (i.e. change in cultivated crops) or harvest, both factors being able to influence soil composition and its organic matter content. It was not possible to gather data on flowers cultivation and livestock, which have been significantly affected by lockdown restrictions according to the Regional Institute for economic planning of Tuscany (http://www.irpet.it).

3.3. The lockdown impact on DOC concentration

In order to test our hypothesis that the removal of a significant fraction of human activities affected DOM dynamics, the data collected in 2020 and 2021 (sampling 2 in the methods) have been compared with those measured in 2014 and 2015 (Retelletti Brogi et al., 2020). The published data on DOC and DOM optical properties (absorption and fluorescence) represent a reference point for DOM dynamics in the river in "normal" conditions, which includes contrasting hydrological conditions. Their comparison with the data collected in 2020–2021 therefore allows to identify changes mostly ascribable to the lockdown.

DOM dynamics in 2020–2021, similarly to 2014 and 2015 (Retelletti Brogi et al., 2020), showed a clear seasonality with the lowest DOC values in winter and a marked increase in spring, in correspondence with the increase in temperature, to reach its maximum in summer (Fig. 3). During the lockdown (April 24th to May 12th, 2020) DOC values (189 ± 8 μM) were significantly lower (−27%) than those observed in 2014 and 2015 during the same period (258 ± 17 μM, and 261 ± 21 μM, respectively; Fig. 3). This difference slightly increased in summer (June and July) reaching −30% of DOC concentration with respect to 2014 and 2015. From August, the difference with the previous years was less marked, although a 21% reduction in DOC concentration was still observed between October and December 2020 (Fig. 3), when a partial lockdown was again established. These results clearly show an offset in DOC concentration between April and December 2020 with respect to previous years, even if the cycle followed the expected seasonal variability. Since December 2020, DOC values were comparable to the pre-lockdown ones (Fig. 3).

A stepwise regression was carried out to test whether the observed decrease in DOC concentration was a consequence of the human activity reduction following the lockdown. This analysis identified 7 factors that explain the variability of DOC in the Arno River (Table S2). Among the selected factors, the average discharge of the 90 days before the sampling is the most significant variable followed by a dummy variable for the period March–July 2021 (p-value in Table S2). These two terms have both a negative impact on DOC concentration (coefficient of the regression model in Table S2). The next two most important variables are the water temperature and the 2-day run-off that represent the positive factors associated with autochthonous DOC production and flood events, respectively. Two other variables, the 30-day run-off average and a second dummy variable for the Aug-Nov 2020 period, contribute negatively to the reconstruction of the DOC variability even if with a lower effect than the other variables. Finally, the degradation of DOC due to the HP has a low marginal effect, indeed the HPA is the last variable to be included in the regression model. Other variables have been excluded from the final regression model given their low level of significance (p-values>0.05; Table S2). The final regression model reconstructs remarkably well the DOC time series (Fig. 4), reproducing the interannual, seasonal, and most of the high-frequency variability with an error of ≈39 μM.

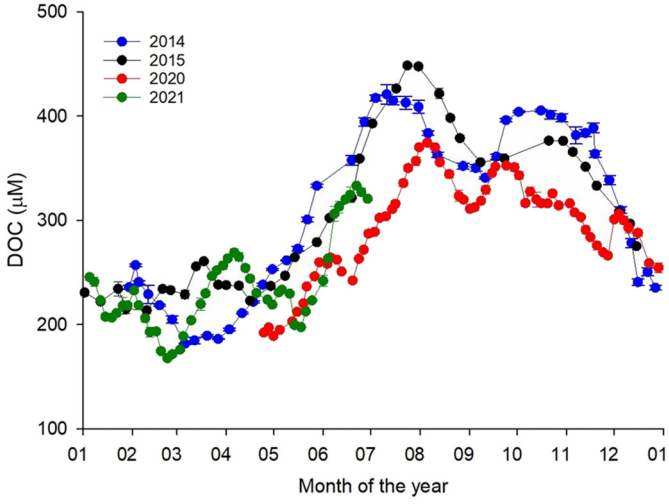

Fig. 3. Arno River DOC concentration in 2014, 2015, 2020, and 2021, bars represent the standard deviation (n = 3). (For interpretation of the references to colour in this figure legend, the reader is referred to the web version of this article.)

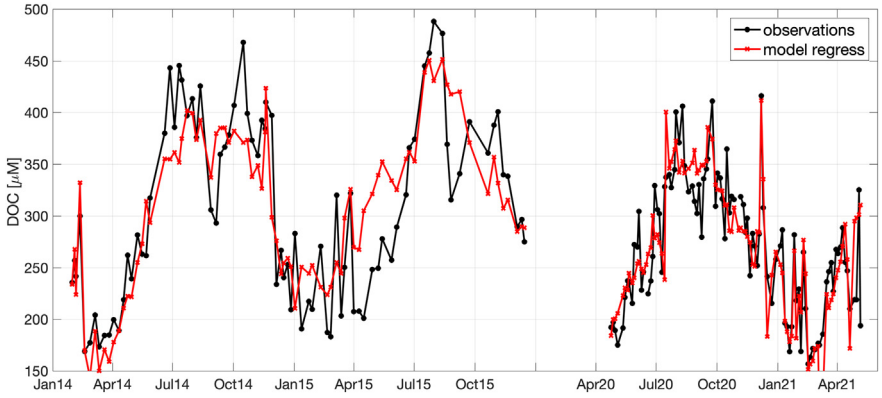

Fig. 4. Time series of DOC observations (black) and values reconstructed by using the stepwise regression model (red). (For interpretation of the references to colour in this figure legend, the reader is referred to the web version of this article.)

3.4. Effects on DOM quality

In agreement with DOC, the absorption coefficient at 254 nm (a_{254}), showed a significant reduction (−26%) during the lockdown (April 24th to May 12th, Fig. S9). During the rest of the year, this difference was reduced, except for July and August when a reduction of 11-16% was still observed with respect to 2014 and 2015. Compared to the previous years, the CDOM spectral slope, $S_{275–295}$, indicates a change in the average molecular weight and aromaticity of the molecules in the CDOM pool. In particular, between April and December 2020, $S_{275–295}$ was higher than in 2014 (on average + 14%) and 2015 (on average + 8%) (Fig. 5). The higher values of $S_{275–295}$ suggest the predominance in the DOM pool of molecules that are smaller and less aromatic in 2020 than in 2014 and 2015. Moreover, the observed $S_{275–295}$ decrease between June and July 2020 suggests a change in DOM molecular properties. Since December 2020, $S_{275–295}$ realigns to the values observed in 2014 and 2015, as observed for DOC.

Fluorescence data further support the change in DOM quality. The total fluorescence normalized by DOC showed values lower in 2020 and at the beginning of 2021 than in 2014 and 2015; from March 2021 the values are comparable to those observed in 2015 (Fig. 5). The largest difference (−41 to –46%) was observed between May and August 2020.

To better evaluate changes in FDOM, a PCA analysis was carried out on the 6 fluorescent components (Fig. 6).

The score of the first two principal components, which explain up to 76% of the total variances, show a marked difference in the fluorescence properties of DOM in 2020–2021 compared to 2014–2015. The 2020–2021 data are grouped in an opposite quadrant with respect to 2014–2015 data (Fig. 6). The first component (PC1) is a positive combination of all fluorescent components except $C5_f$, while the second component (PC2) is a positive combination of $C1_{mh}$, $C4_p$, and $C5_f$ with a lower and negative contribution from $C2_{th}$, $C3_f$, $C6_{pah}$ (Fig. 6). Thus, it emerges that $C1_{mh}$ and $C4_p$, contribute equally to PC1 and PC2, having no particular influence on the distribution of the samples. On the other hand, $C2_{th}$, $C3_f$, and $C6_{pah}$, in opposition with $C5_f$, drive the observed separation of the 2014–2015 and 2020–2021 samples in the first two components projection.

The distribution of the samples is also reflected in the annual dynamics of these components in 2020–2021 (Fig. S10). Both components $C3_f$ and $C5_f$ can be identified as fulvic-like, having only a small shift in excitation and emission maxima (Fig. S6, Table S1). The small blue shift in excitation and emission maxima of $C5_f$ with respect to $C3_f$ suggests that $C5_f$ fluorophores are on average smaller and less aromatic than $C3_f$ fluorophores. These two components have an opposite behavior in 2020–2021 with respect to 2014–2015; $C3_f$ fluorescence is strongly reduced in 2020–2021 with respect to 2014–2015, whereas $C5_f$ was markedly higher in 2020-2021 than in 2014–2015, when it showed a very low fluorescence (Fig. S10). These data suggest that the fulvic-like compounds present in 2014–2015 were replaced by similar but smaller and less aromatic compounds in 2020. These results are in agreement with the high values of $S_{275–295}$ observed in 2020. Component $C6_{pah}$, attributed to polycyclic aromatic hydrocarbons-like molecules, showed one of the biggest differences among years, being reduced by 72 to 92% in 2020 with respect to 2014 and 2015, respectively.

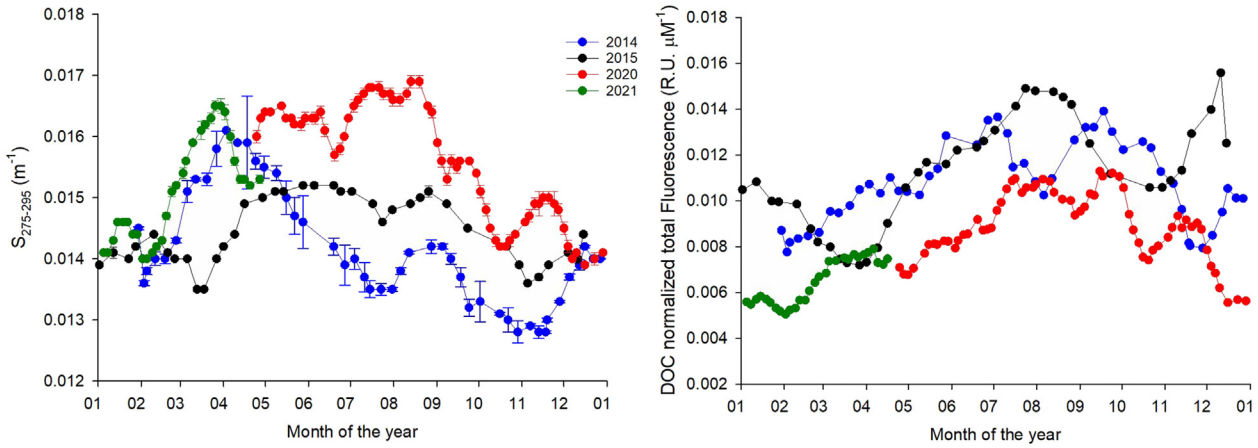

Fig. 5. Arno River CDOM spectral slope ($S_{275–295}$) in 2014, 2015, 2020, and 2021 (left panel), error bars represent the standard deviation (n = 3); Arno River DOC normalized total fluorescence in 2014, 2015, 2020, and 2021 (right panel). (For interpretation of the references to colour in this figure legend, the reader is referred to the web version of this article.)

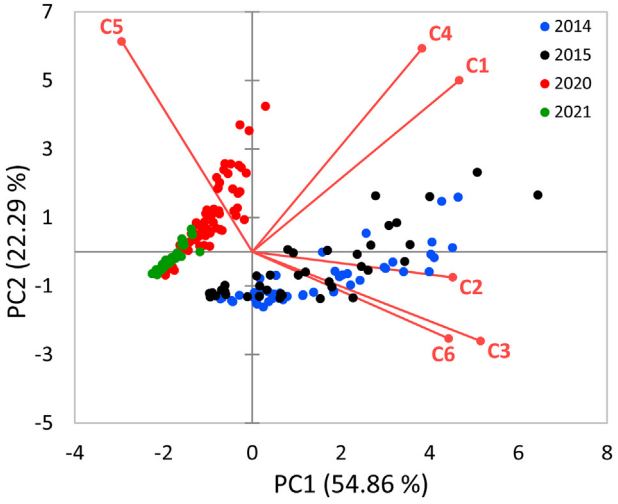

Fig. 6. Results of the PCA carried out on fluorescence data. Red lines and dots refer to loadings and scores of the first two principal components. The colors of the symbols identify the sampling year. (For interpretation of the references to colour in this figure legend, the reader is referred to the web version of this article.)

3.5. The change in DOM dynamics affected the microbial loop

Since HP are the main consumers of DOM, their abundance was used to evaluate if and how changes in DOM dynamics affected the microbial loop, also inferring a potential impact on the higher trophic levels. In 2014 and 2015, HPA gradually increased from May (Fig. 7), showing a linear correlation with water temperature (Retelletti Brogi et al., 2020). Differently, in 2020, HPA did not increase until the end of June, when a sudden, sharp increase was observed in a very short time (Fig. 7). This HPA maximum persisted for 1 month and coincided with the change in $S_{275–295}$ (Fig. 5). Both $C1_{mh}$ and $C4_{p}$ components increased in correspondence with the peak in HPA (Fig. S10). This observation suggests that the low HPA values, measured before July 2020, may have been caused by the presence of a qualitatively different DOM, which is also reflected in a coincident relative increase in the High Nucleic Acid (HNA) subpopulation (Santos et al., 2019), indicating a shift in the prokaryotic community composition (Fig. S11). Before July, the HPA lower in 2020 than in 2014 and 2015 may therefore have determined a reduced transfer of energy to the higher trophic levels, whereas between July and Octber 2020, HPA was markedly higher than in previous years.

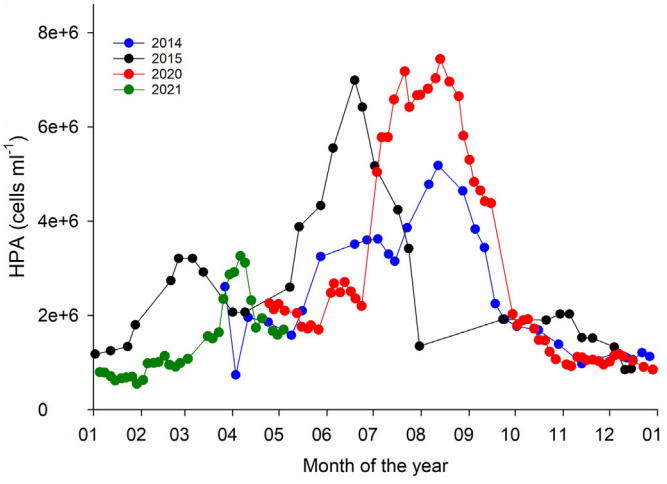

Fig. 7. Annual trend of the heterotrophic prokaryotes abundance (HPA) in 2014, 2015, 2020, and 2021. (For interpretation of the references to colour in this figure legend, the reader is referred to the web version of this article.)

3.6. Impact of the lockdown on the coastal area

The marked reduction in DOC, observed in the river between April and August 2020, resulted in a decrease in the total DOC flux to the coastal area. The average daily DOC flux during this period ($5.9 \cdot 10^6$ g DOC day^{-1}) was indeed 58% less than in 2014 ($1.4 \cdot 10^7$ g DOC day^{-1}), with average daily water discharg 43% lower. The impact was much more striking with respect to 2015 ($8.6 \cdot 10^6$ g DOC day^{-1}) when a 31% reduction of DOC flux was observed despite a reduction of the average daily water discharg of only 16%.

The observed DOC reduction in the Arno River is also mirrored by the very low DOC concentration in front of the river mouth (Fig. S12) during the lockdown. DOC concentration, measured in 15 stations within 12 miles from the coast (Fig. 1), was 58 ± 3 μM (range = 48–62 μM; Fig. S12). These values are 15% lower than data collected in the same area between 1998 and 2015, showing an average DOC concentration of 68 ± 5 μM over different seasons (Retelletti Brogi et al., 2015).

Satellite images show a marked reduction in the Chl-a concentration, with respect to the 2016–2019 climatology (Fig. 8). In particular, it is evident a consistent decrease in the weekly Chl-a concentration anomaly from 1 April to 12 May 2020. It is noteworthy that the most marked anomaly (dark area in Fig. 8) is coherent with the main path of the Arno River plume (moving northward the estuary). This clearly indicates that the coastal pattern of Chl-a concentration during the lockdown was strongly controlled by the coastal plume dynamic, which connects inland water inputs with the coastal marine environment. The low DOC concentration in the coastal area could be a combination of a low input by the Arno River and a low in-situ production, probably due to a low riverine input of nutrients.

4. Discussion

4.1. How do human activities impact the riverine DOM dynamics?

The 125 μM DOC enrichment, observed from the spring to the mouth of the Arno River in March 2021, can be mostly attributed to allochthonous sources, being in-situ production at its minimum (Retelletti Brogi et al., 2020). Being riverine DOM an integrated result of natural and anthropic inputs and the physico-chemical and biological re-elaboration of these inputs within the soil, the river itself and the processes occurring in the watershed, its potential sources can be only determined indirectly. In addition, within the soil the transformation mechanisms affecting the concentration and properties of the DOM finally transferred into the rivers are poorly known, and a chemical characterization of DOM both in the soil and in the water is still missing. For all these reasons, it is not possible to quantify the anthropogenic inputs and so far there is no way to disentangle the contribution of the different sources to riverine DOM.

The interruption of a large number of human activities during the lockdown, in particular industries and transportations (Fig. S8), is therefore expected to influence DOC dynamics in the river. Indeed, the comparison of our data with those collected in 2014–2015, combined with the stepwise analysis, provides a robust evidence that the restriction to the human activities significantly reduced the DOC concentration in the river (Figs. 3 and 4) and changed its optical properties (Figs. 5, 6, S9, and S10). The stepwise analysis allowed to quantify a riverine DOC reduction of 130 and 20 μM, corresponding to 44% and 7% of the mean annual concentration, in 2 periods. The first period is between April and July 2020, corresponding to the almost complete restriction to human activities during the first phase of the COVID-19 pandemic and their partial relief in the following 2 months; the second period is between August and November 2020, corresponding to the recovery of some activities, but with still many restrictions, especially for tourism and transportation, as shown from the mobility data (Fig. S8d). It is, therefore, reasonable to state that at least 130 μM of DOC

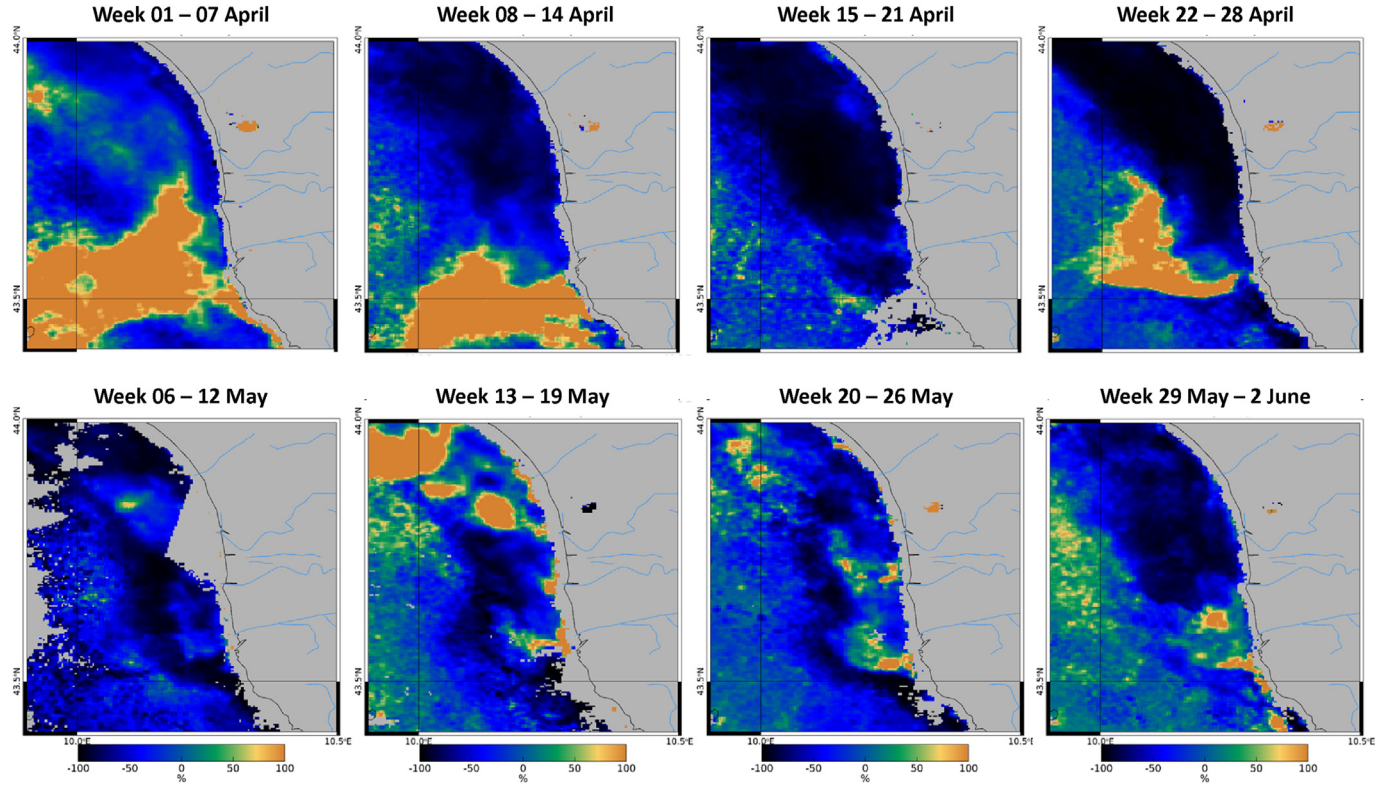

Fig. 8. Weekly Chlorophyll-a concentration anomaly in the area in front of the Arno River mouth. The week 22–28 April and the week 6–12 May correspond to the week before and the week after the sampling. Data from the sampling week are not available due to cloud cover. (For interpretation of the references to colour in this figure legend, the reader is referred to the web version of this article.)

in the river (those reduced during the strong lockdown) are due to anthropic activities. The link between DOC reduction and lockdown is further supported by the "recovery" of the system to its pre-lockdown conditions since December 2020, when most of the restrictions were relieved, as also shown by the rejection of the other dummy variables (Table S2).

It is important to stress that, from a climatic point of view, 2020 was not significantly different from the average conditions (i.e., 2004–2021 climatology, Figs. S13, and S14), thus excluding environmental factors as drivers of the observed changes in DOM dynamics.

One of the main effects of the marked reduction in industrial activities and transportations was a noticeable improvement in air quality (Elsaid et al., 2021). Industrial activities, as well as rail, road, and air traffic, contribute to organic carbon through particulate matter (PM) emission into the atmosphere (Chow et al., 2011). The improvement of the air quality could have therefore had an important role in the observed reduction of riverine DOC, being the atmospheric deposition an important and overlooked source of DOC to the Mediterranean area (Galletti et al., 2020). Atmospheric organic carbon can reach the riverine water both directly by atmospheric deposition on the water and indirectly by the deposition on land and vegetation which can be then flushed to the river by the rain or by an increase in the water level. In order to roughly estimate the contribution of atmospheric deposition to the DOC pool in the Arno River before the lockdown, we assume that the range of its concentration in atmospheric deposition reported in the literature over the Mediterranean area (59–153 m mol C m^{-2} yr^{-1}; de Vicente et al., 2012; Djaoudi et al., 2018; Galletti et al., 2020; Pulido-Villena et al., 2008) is valid for the Arno River drainage basin ($8.23{\cdot}10^9$ m^2). This calculation indicates a flux ranging between 16 and $41{\cdot}10^6$ g C day^{-1} (5.8 and $15.1{\cdot}10^9$ g C yr^{-1}). These values are very similar to the total DOC flux from the Arno River to the Mediterranean Sea ($5.1–12.9 \cdot 10^9$ g C yr^{-1}) (Retelletti Brogi et al., 2020). To the best of our knowledge, there is no information about the percentage of atmospheric organic carbon deposited over the river drainage basin reaching riverine water. It would be crucial to quantify the amount of atmospheric DOC that reaches the river since, even if we assume that only 10% will reach the river, this input would increase riverine DOC concentration by 17–46 μM, supporting the relevance of this source. It is important to stress that these values are probably underestimated since the data reported in the literature mostly refer to remote sites, whereas the river drainage basin is highly affected by anthropic activities. A reduction of 45% of atmospheric black carbon (i.e. the carbon produced by incomplete combustion) due to the lockdown was observed in Spain (Tobías et al., 2020). Assuming a reduction of atmospheric OC similar to that observed in Spain, the lockdown could have caused a $6–16{\cdot}10^6$ g C day^{-1}reduction in atmospheric deposition to the river drainage basin. The reduced input of anthropogenic DOM from the atmosphere is also supported by the marked reduction in $C6_{pah}$ (Fig. S10); this component is attributed to the presence of PAHs, commonly found in rivers worldwide because of anthropogenic activities (Mojiri et al., 2019). As PHAs are big aromatic compounds, a decrease in their abundance is also supported by the decrease in the average aromaticity of the molecules indicated by the increase in $S_{275–295}$.

The marked reduction in industrial activities in Tuscany (Fig. S8a) may also have a direct effect on DOM in the river due to the reduced wastewater discharge. Most of the industries have wastewater treatment plants; data about the amount and the kind of compounds discharged into the river are not available, making very difficult to quantify these inputs and their reduction due to the COVID-19 lockdown. Nevertheless, it is known that the most water-polluting industries, in terms of organic contamination, are those dealing with organic raw materials (UNWWAP, 2003) (e.g. food, drinks, paper, and textile industries), which are abundant in the Arno River basin.

The observed shift toward a smaller and less aromatic DOM pool (i.e. higher spectral slope, Fig. 5), the decrease in total fluorescence (Fig. 5), and the changes in the fulvic and PAH-like components (Fig. S10) are difficult to compare with other studies. Human activities can have contrasting effects on riverine DOM, they can either increase or decrease the average molecular weight and aromaticity, and these effects are highly context-

dependent and variable on a local and regional scale, according to the characteristics of the watershed (Xenopoulos et al., 2021). The effect of human disturbance on DOM properties is indeed influenced by several factors, such as soil structure, lithology, climate, vegetation cover, population density, crops type, industrial activity (Lambert et al., 2017; Xenopoulos et al., 2021).

Tourism may have had a direct effect on riverine DOM through the decrease in sewage organic load ascribable to the presence of fewer people over a certain area with respect to previous years. The effect of this reduced sewage input on DOC concentration is probably not visible since sewage mostly brings labile DOM (Regnier et al., 2013). It is therefore probable that this contribution is not measurable since it is rapidly removed, as it can be observed from the lack of DOC enrichment after the city of Florence (Fig. 2). It is possible to hypothesize that the reduction of labile DOM may have contributed to the low HPA until July since HP had less labile DOM to use for their growth. Tourism can also have important indirect effects on DOM reduction by influencing both traffic and agriculture; fewer tourists mean less transportation as well as reduced food needs.

4.2. Changed DOM dynamics: implication for the riverine and coastal ecosystems

Considering that DOC in Mediterranean rivers ranges between 92 and 500 μM (Retelletti Brogi et al., 2020; Santinelli, 2015), and between 36 and 90 μM in both the Mediterranean Sea and the global ocean (Roshan and DeVries, 2017; Santinelli, 2015), the observed decrease in the Arno River (up to 130 μM) is highly significant. Due to its complex nature (i.e. numerous sources and transformation processes) and its multiple interaction within the aquatic environment, it cannot be stated weather this marked reduction in DOC had an overall positive or a negative effect on the riverine ecosystem and the coastal area. Yet some positive effects can be highlighted, with the support of the results shown in previous studies.

1. In the river, the reduced DOM concentration and the different quality impacted the microbial loop:

   a. The reduced HPA until July and the delay in the HP growth in 2020 with respect to the previous years, might result in a reduction of microbial respiration rates, reducing the CO_2 released into the atmosphere. This is further supported by the shift in HNA bacteria within the community (Fig. S11). Taking into account the decrease in DOC and the lower HPA observed between April and July 2020 than in 2014–2015, one can estimate the decrease in CO_2. Assuming that all the missing DOC was labile (and therefore consumed by the HP community in a relatively short time), and taking into account the HP growth efficiency (HPGE) calculated for the Arno River estuary (Retelletti Brogi et al., 2021), it is possible to estimate a 2.4–7.6 · 10^6 g C day^{-1} decrease in the CO_2 released into the atmosphere in 2020 compared to 2014 and 2015. This calculation may however overestimate the reduction in CO_2 fluxes, due to the assumption that all the missing DOC is labile and therefore entirely uptaken by the HP. Another way to estimate the "missing CO_2 production" is to use the HPA abundance and indirectly retrieve the HP carbon demand (HPCD) by using the Arno HPGE (Retelletti Brogi et al., 2021). These calculations indicate a reduction of the CO_2 flux to the atmosphere of 0.5–3.0 · 10^6 g C day^{-1} compared to 2014–2015.
   b. Between July and October 2020, a much higher HPA, together with a longer persistence of its maximum (i.e. almost 2 months), was observed with respect to 2014 and 2015 (Fig. 7). An increased biomass when the resources (i.e. DOM, Fig. 3) are reduced is surprising. The explanations can be several and would need further investigation, but with the available data, it was possible to observe a change in DOM quality in 2020. This suggests that a higher fraction of the 2020 DOM was used to build biomass instead of being used for respiration, leading to a possible increase in the energy transfer to the higher trophic levels;
2. The reduction in DOM together with its different quality could increase microbial diversity in both the river and the estuary. It has indeed been observed that the composition of the microbial community and its functioning vary according to the composition of the DOM pool (Logue et al., 2016; Osterholz et al., 2016; Xenopoulos et al., 2021). DOM composition has been also demonstrated to affect primary production (Creed et al., 2018; Kelly et al., 2018; Xenopoulos et al., 2021) and alter ecosystem respiration rates and metabolism (Jane and Rose, 2018). The satellite analysis, indeed, revealed that the anomalous pattern of Chl-a concentration along the coastal area was significantly affected by the buoyancy Arno River plume (Fig. 8), which showed a coherent alongshore dynamic. Anomalies of Chl-a concentration, which represents the most direct indicator of phytoplankton biomass in coastal environments, were likely connected to riverine inputs (Colella et al., 2016). An increase in bacterial diversity due to the lockdown restrictions has been observed also in the Godavari River (India, Jani et al., 2021).
3. In both the riverine and coastal environment, a reduction of DOM, in particular of humic-like substances, will reduce the ability of DOM to complex pollutants and metals, leading to lower bioavailability of these substances. It has indeed been observed that the increase in DOC concentration is correlated to a higher bioavailability of metals and pollutants to both bacteria (Aiken et al., 2011; Chiasson-Gould et al., 2014; Pothier et al., 2020) and bigger organisms (Bourdineaud et al., 2019), and to a higher production of toxic compounds such as methylmercury (Bravo and Cosio, 2020), favoring their bioaccumulation in the higher trophic levels and posing a threat to human health.
4. The complexation between DOM and metals is also an important issue in those regions where riverine water is the source for drinking water production (Matilainen et al., 2011). DOM concentration is correlated with the production of toxic disinfection by-products (DBPs) during chlorination (Zhang et al., 2020), a fundamental step in water treatment plants. A decrease in DOM concentration would therefore simplify the drinking water treatment, increasing the efficiency and reducing the cost.
   A 31–58% reduction in DOC flux from the river could be highly beneficial for the coastal area. It has indeed been shown that a high load of terrestrial DOM might advantage heterotrophs (Andersson et al., 2013; Wikner and Andersson, 2012), causing a shift in the composition of the biological community, that can ultimately lead to a net heterotrophy of the system (Deininger and Frigstad, 2019). This condition (i.e., increase in respiration and decrease in oxygen production) can increase the release of greenhouse gases and favor processes such as (i) hypoxia (Andersson et al., 2013; Lapierre et al., 2013; Wikner and Andersson, 2012), (ii) changes in benthic and pelagic community composition (Deininger et al., 2017; Jessen et al., 2015; Moy and Christie, 2012), and (iii) reduced efficiency in energy transfer to higher trophic levels (Deininger and Frigstad, 2019).

5. Conclusions and perspectives

The unfortunate circumstances of the lockdown due to the COVID-19 pandemic allowed to observe a period of strongly reduced anthropogenic pressure. For the first time, it was possible to grab a snapshot of an almost background condition which provided an estimate of the real impact that human activities can have on the riverine and coastal environments.

Our data not only show the first evidence of the impact of the lockdown on DOM dynamics in rivers, but also allowed to quantify for the first time that at least 44% of DOM in the Arno River is ascribable to human-related activities, mostly from secondary and tertiary sectors, stopped during the lockdown. This percentage is astounding and indicates that a very large fraction of DOM in this small river does not come from 'natural' processes, but from anthropic activities. This percentage is probably higher because it does not include the reduction of sewage (mostly biological labile DOC) due to the much lower number of tourists.

The high temporal resolution sampling (two times per week) together with the detailed, parallel analysis of the climate components (i.e. discharge, precipitation, temperature) as well as of the biomass indicator

(chlorophyll-a in the coastal area), allowed us to discriminate the effect of the lockdown from single disturbance events that could affect the DOM dynamics on the short temporal scale.

Moreover, our study gives insights into the impact of lockdown to the ecosystem, bringing evidences that the change in both DOM concentration and quality affected the abundance and trend of heterotrophic prokaryotes, that are a key component of the riverine ecosystem, starting the microbial loop.

Finally, by covering up to 1 year after the lockdown (from April 2020 to May 2021), our results show the return of the system to pre-lockdown conditions, supporting on one hand the link between the observed changes and the temporary stop of the anthropogenic activities, on the other hand the short-time effect that the lockdown had on the ecosystem (i.e. approximately 6 months to go back to pre-lockdown conditions). Even though further studies, aimed at a better quantification of the external inputs and their effects on the riverine biological community, are surely needed, it is evident that many of the putative anthropogenic sources that contribute to riverine DOM could be kept under tighter control even after a back-to-normal of human activities. The observed short time needed to the riverine DOM to return to pre-lockdown conditions even with a not full relaunch of the activities, highlights that such a strong reduction of anthropogenic pressure for a short period can give very limited beneficial effects to the riverine ecosystem. This suggests that different, even small yet constant, practices can be suggested in order to reduce the impact of human activities on the river. For instance, exhaust can be filtered, DOM in industrial wastewater could be better treated, anthropogenic DOM release in the atmosphere could be better controlled. All the above would drive small rivers toward a status likely closer to a sustainable regime than that regularly observed before the lockdown.

Thanks to their rapid response to environmental changes, small rivers can be considered as sentinels and used to investigate the effects of restorations actions as well as the effect of global changes and human activities. Our work also stresses the importance of long-term research on key areas in order to disentangle the effects of casual events from natural variability.

CRediT authorship contribution statement

S. Retelletti Brogi: Conceptualization, Formal analysis, Investigation, Methodology, Visualization, Data curation, Writing – original draft. **G. Cossarini:** Formal analysis, Investigation, Data curation, Visualization, Writing – review & editing. **G. Bachi:** Investigation, Writing – review & editing. **C. Balestra:** Formal analysis, Investigation, Writing – review & editing. **E. Camatti:** Investigation, Writing – review & editing. **R. Casotti:** Formal analysis, Investigation, Resources, Data curation, Writing – review & editing. **G. Checcucci:** Investigation, Writing – review & editing. **S. Colella:** Formal analysis, Visualization, Investigation, Writing – review & editing. **V. Evangelista:** Investigation. **F. Falcini:** Investigation, Visualization, Writing – review & editing. **F. Francocci:** Formal analysis, Data curation. **T. Giorgino:** Formal analysis, Data curation, Writing – review & editing. **F. Margiotta:** Investigation, Resources, Data curation, Writing – review & editing. **M. Ribera d'Alcalà:** Conceptualization, Writing – review & editing. **M. Sprovieri:** Conceptualization, Writing – review & editing, Project administration. **S. Vestri:** Investigation. **C. Santinelli:** Conceptualization, Investigation, Data curation, Formal analysis, Methodology, Resources, Writing – review & editing, Project administration, Funding acquisition.

Declaration of competing interest

The authors declare that they have no known competing financial interests or personal relationships that could have appeared to influence the work reported in this paper.

Acknowledgment

This research was supported by the SNAPSHOT (Synoptic Assessment of Human Pressures on key Mediterranean Hot Spots) project, funded by the Department of Earth System Science and Environmental Technologies, CNR (Italy). We thank Nunzia Antonicelli, Marco Carloni, Claudia Tropea and Silvia Valsecchi for their support in the Arno river weekly sampling and samples filtration and analyses. We are grateful to Margherita Gonnelli for her scientific support. We further thank Davide Pellegrini for his help with GIS data, and Tommaso Ferraresi for industrial production data. Particular thanks are due to the Centro Interuniversitario di Biologia Marina "G.Bacci" for its support in the coastal sampling. The satellite analysis was carried out as part of the SOON (Satellite Observations for inland and cOastal water quality during COVID lock-dowN) project, funded by the European Space Agency via the contract Grant No. 4000128147/19/I-DT.

Appendix A. Supplementary data

Supplementary data to this article can be found online at https://doi.org/10.1016/j.scitotenv.2021.152412.

References

Aiken, G.R., Hsu-Kim, H., Ryan, J.N., 2011. Influence of dissolved organic matter on the environmental fate of metals, nanoparticles, and colloids. Environ. Sci. Technol. 45, 3196–3201. https://doi.org/10.1021/es103992s.

Andersson, A., Jurgensone, I., Rowe, O.F., Simonelli, P., Bignert, A., Lundberg, E., Karlsson, J., 2013. Can humic water discharge counteract eutrophication in coastal Waters? PLoS One 8, e61293. https://doi.org/10.1371/journal.pone.0061293.

Aufdenkampe, A.K., Mayorga, E., Raymond, P.A., Melack, J.M., Doney, S.C., Alin, S.R., Aalto, R.E., Yoo, K., 2011. Riverine coupling of biogeochemical cycles between land, oceans, and atmosphere. Front. Ecol. Environ. 9, 53–60. https://doi.org/10.1890/100014.

Balestra, C., Alonso-Sáez, L., Gasol, J.M., Casotti, R., 2011. Group-specific effects on coastal bacterioplankton of polyunsaturated aldehydes produced by diatoms. Aquat. Microb. Ecol. 63, 123–131. https://doi.org/10.3354/ame01486.

Bourdineaud, J.-P., Gonzalez-Rey, M., Rovezzi, M., Glatzel, P., Nagy, K.L., Manceau, A., 2019. Divalent mercury in dissolved organic matter is bioavailable to fish and accumulates as dithiolate and tetrathiolate complexes. Environ. Sci. Technol. 53, 4880–4891. https://doi.org/10.1021/acs.est.8b06579.

Bravo, A.G., Cosio, C., 2020. Biotic formation of methylmercury: a bio–physico–chemical conundrum. Limnol. Oceanogr. 65, 1010–1027. https://doi.org/10.1002/lno.11366.

Carlson, R.E., Fritsch, F.N., 1989. An algorithm for monotone piecewise bicubic interpolation. SIAM J. Numer. Anal. 26, 230–238. https://doi.org/10.1137/0726013.

Carlson, C.A., Hansell, D.A., 2015. DOM sources, sinks, reactivty, and budgets. Biogeochemistry of Marine Dissolved Organic Matter, pp. 65–126 https://doi.org/10.1016/B978-0-12-405940-5.00003-0.

Chiasson-Gould, S.A., Blais, J.M., Poulain, A.J., 2014. Dissolved organic matter kinetically controls mercury bioavailability to bacteria. Environ. Sci. Technol. 48, 3153–3161. https://doi.org/10.1021/es4038484.

Chow, J.C., Watson, J.G., Lowenthal, D.H., Antony Chen, L.-W., Motallebi, N., 2011. PM2.5 source profiles for black and organic carbon emission inventories. Atmos. Environ. 45, 5407–5414. https://doi.org/10.1016/j.atmosenv.2011.07.011.

Colella, S., Falcini, F., Rinaldi, E., Sammartino, M., Santoleri, R., 2016. Mediterranean Ocean colour chlorophyll trends. PLoS One 11, e0155756. https://doi.org/10.1371/journal.pone.0155756.

Cortecci, G., Boschetti, T., Dinelli, E., Cidu, R., Podda, F., Doveri, M., 2009. Geochemistry of trace elements in surface waters of the Arno River Basin, northern Tuscany, Italy. Appl. Geochemistry https://doi.org/10.1016/j.apgeochem.2009.03.002.

Creed, I.F., Bergström, A.-K., Trick, C.G., Grimm, N.B., Hessen, D.O., Karlsson, J., Kidd, K.A., Kritzberg, E., McKnight, D.M., Freeman, E.C., Senar, O.E., Andersson, A., Ask, J., Berggren, M., Cherif, M., Giesler, R., Hotchkiss, E.R., Kortelainen, P., Palta, M.M., Vrede, T., Weyhenmeyer, G.A., 2018. Global change-driven effects on dissolved organic matter composition: implications for food webs of northern lakes. Glob. Chang. Biol. 24, 3692–3714. https://doi.org/10.1111/gcb.14129.

Deininger, A., Frigstad, H., 2019. Reevaluating the role of organic matter sources for coastal eutrophication, oligotrophication, and ecosystem health. Front. Mar. Sci. 6, 210.

Deininger, A., Faithfull, C.L., Bergström, A.-K., 2017. Phytoplankton response to whole lake inorganic N fertilization along a gradient in dissolved organic carbon. Ecology 98, 982–994. https://doi.org/10.1002/ecy.1758.

Del Vecchio, R., Blough, N.V., 2004. Spatial and seasonal distribution of chromophoric dissolved organic matter and dissolved organic carbon in the middle Atlantic bight. Mar. Chem., 169–187 https://doi.org/10.1016/j.marchem.2004.02.027.

Development Core, Team R., 2018. A Language and Environment for Statistical Computing. R Found. Stat. Comput.

Djaoudi, K., Van Wambeke, F., Barani, A., Hélias-Nunige, S., Sempéré, R., Pulido-Villena, E., 2018. Atmospheric fluxes of soluble organic C, N, and P to the Mediterranean Sea: potential biogeochemical implications in the surface layer. Prog. Oceanogr. 163, 59–69. https://doi.org/10.1016/j.pocean.2017.07.008.

Draper, N.R., Harry, Smith, 1998. Selecting the "best" regression equation. In: Draper, N.R., Harry, Smith (Eds.), Applied Regression Analysis. John Wiley & Sons, Inc, pp. 327–368.

Dutta, V., Dubey, D., Kumar, S., 2020. Cleaning the river ganga: impact of lockdown on water quality and future implications on river rejuvenation strategies. Sci. Total Environ. 743, 140756. https://doi.org/10.1016/j.scitotenv.2020.140756.

Elsaid, K., Olabi, V., Sayed, E.T., Wilberforce, T., Abdelkareem, M.A., 2021. Effects of COVID-19 on the environment: an overview on air, water, wastewater, and solid waste. J. Environ. Manag. 292, 112694. https://doi.org/10.1016/j.jenvman.2021.112694.

Galletti, Y., Becagli, S., di Sarra, A., Gonnelli, M., Pulido-Villena, E., Sferlazzo, D.M., Traversi, R., Vestri, S., Santinelli, C., 2020. Atmospheric deposition of organic matter at a remote site in the Central Mediterranean Sea: implications for the marine ecosystem. Biogeosciences 17, 3669–3684. https://doi.org/10.5194/bg-17-3669-2020.

Hansell, D.A., 2005. Dissolved organic carbon reference material program. EosTrans. Am. Geophys. Union 86, 318. https://doi.org/10.1029/2005EO350003.

IRPET, 2020. La situazione economica, il lavoro e le disuguaglianze in Toscana ai tempi del Covid-19.

Jane, S.F., Rose, K.C., 2018. Carbon quality regulates the temperature dependence of aquatic ecosystem respiration. Freshw. Biol. 63, 1407–1419. https://doi.org/10.1111/fwb.13168.

Jani, K., Bandal, J., Shouche, Y., Shafi, S., Azhar, E.I., Zumla, A., Sharma, A., 2021. Extended ecological restoration of bacterial communities in the Godavari River during the COVID-19 lockdown period: a spatiotemporal meta-analysis. Microb. Ecol. 82, 365–376. https://doi.org/10.1007/s00248-021-01781-0.

Jessen, C., Bednarz, V.N., Rix, L., Teichberg, M., Wild, C., 2015. Marine eutrophication. In: Armon, R.H., Hänninen, O. (Eds.), Environmental Indicators. Springer, Netherlands, Dordrecht, pp. 177–203 https://doi.org/10.1007/978-94-017-9499-2_11.

Kelly, P.T., Solomon, C.T., Zwart, J.A., Jones, S.E., 2018. A framework for understanding variation in pelagic gross primary production of Lake ecosystems. Ecosystems 21, 1364–1376. https://doi.org/10.1007/s10021-018-0226-4.

Lakowicz, J.R., 2006. Quenching of fluorescence, principles of fluorescence. Spectroscopy, 277–330 https://doi.org/10.1007/978-0-387-46312-4_8.

Lambert, T., Bouillon, S., Darchambeau, F., Morana, C., Roland, F.A.E.E., Descy, J.-P.P., Borges, A.V., 2017. Effects of human land use on the terrestrial and aquatic sources of fluvial organic matter in a temperate river basin (The Meuse River, Belgium). Biogeochemistry 136, 191–211. https://doi.org/10.1007/s10533-017-0387-9.

Lapierre, J.-F., Guillemette, F., Berggren, M., Del Giorgio, P.A., 2013. Increases in terrestrially derived carbon stimulate organic carbon processing and CO2 emissions in boreal aquatic ecosystems. Nat. Commun. 4, 2972. https://doi.org/10.1038/ncomms3972.

Legendre, P., Legendre, L., 2012. Ordination in reduced space. In: Legendre, P., Legendre, L. (Eds.), Numerical Ecology. Elsevier B.V, pp. 425–520.

Logue, J.B., Stedmon, C.A., Kellerman, A.M., Nielsen, N.J., Andersson, A.F., Laudon, H., Lindström, E.S., Kritzberg, E.S., 2016. Experimental insights into the importance of aquatic bacterial community composition to the degradation of dissolved organic matter. ISME J. 10, 533–545. https://doi.org/10.1038/ismej.2015.131.

Matilainen, A., Gjessing, E.T., Lahtinen, T., Hed, L., Bhatnagar, A., Sillanpää, M., 2011. An overview of the methods used in the characterisation of natural organic matter (NOM) in relation to drinking water treatment. Chemosphere 83, 1431–1442. https://doi.org/10.1016/j.chemosphere.2011.01.018.

Mojiri, A., Zhou, J.L., Ohashi, A., Ozaki, N., Kindaichi, T., 2019. Comprehensive review of polycyclic aromatic hydrocarbons in water sources, their effects and treatments. Sci. Total Environ. 696, 133971. https://doi.org/10.1016/j.scitotenv.2019.133971.

Moy, F.E., Christie, H., 2012. Large-scale shift from sugar kelp (saccharina latissima) to ephemeral algae along the south and west coast of Norway. Mar. Biol. Res. 8, 309–321. https://doi.org/10.1080/17451000.2011.637561.

Murphy, K.R., Stedmon, C.A., Graeber, D., Bro, R., 2013. Fluorescence spectroscopy and multi-way techniques. PARAFAC. Anal. Methods 5, 6557. https://doi.org/10.1039/c3ay41160e.

Murphy, K.R., Stedmon, C.A., Wenig, P., Bro, R., 2014. OpenFluor- an online spectral library of auto-fluorescence by organic compounds in the environment. Anal. Methods 6, 658–661. https://doi.org/10.1039/C3AY41935E.

Omanović, D., Santinelli, C., Marcinek, S., Gonnelli, M., 2019. ASFit - an all-inclusive tool for analysis of UV–Vis spectra of colored dissolved organic matter (CDOM). Comput. Geosci. https://doi.org/10.1016/j.cageo.2019.104334.

Osterholz, H., Singer, G., Wemheuer, B., Daniel, R., Simon, M., Niggemann, J., Dittmar, T., 2016. Deciphering associations between dissolved organic molecules and bacterial communities in a pelagic marine system. ISME J. 10, 1717–1730. https://doi.org/10.1038/ismej.2015.231.

Patel, P.P., Mondal, S., Ghosh, K.G., 2020. Some respite for India's dirtiest river? Examining the Yamuna's water quality at Delhi during the COVID-19 lockdown period. Sci. Total Environ. 744, 140851. https://doi.org/10.1016/j.scitotenv.2020.140851.

Pothier, M.P., Lenoble, V., Garnier, C., Misson, B., Rentmeister, C., Poulain, A.J., 2020. Dissolved organic matter controls of arsenic bioavailability to bacteria. Sci. Total Environ. 716, 137118. https://doi.org/10.1016/j.scitotenv.2020.137118.

Pulido-Villena, E., Wagener, T., Guieu, C., 2008. Bacterial response to dust pulses in the western Mediterranean: implications for carbon cycling in the oligotrophic ocean. Glob. Biogeochem. Cycles 22. https://doi.org/10.1029/2007GB003091.

Regnier, P., Friedlingstein, P., Ciais, P., Mackenzie, F.T., Gruber, N., Janssens, I.A., Laruelle, G.G., Lauerwald, R., Luyssaert, S., Andersson, A.J., Arndt, S., Arnosti, C., Borges, A.V., Dale, A.W., Gallego-Sala, A., Goddéris, Y., Goossens, N., Hartmann, J., Heinze, C., Ilyina, T., Joos, F., Larowe, D.E., Leifeld, J., Meysman, F.J.R., Munhoven, G., Raymond, P.A., Spahni, R., Suntharalingam, P., Thullner, M., 2013. Anthropogenic perturbation of the carbon fluxes from land to ocean. Nat. Geosci. 6, 597–607. https://doi.org/10.1038/ngeo1830.

Retelletti Brogi, S., Gonnelli, M., Vestri, S., Santinelli, C., 2015. Biophysical processes affecting DOM dynamics at the Arno river mouth (Tyrrhenian Sea). Biophys. Chem. 197, 1–9.

Retelletti Brogi, S., Balestra, C., Casotti, R., Cossarini, G., Galletti, Y., Gonnelli, M., Vestri, S., Santinelli, C., 2020. Time resolved data unveils the complex DOM dynamics in a Mediterranean river. Sci. Total Environ. https://doi.org/10.1016/j.scitotenv.2020.139212.

Retelletti Brogi, S., Casotti, R., Misson, B., Balestra, C., Gonnelli, M., Vestri, S., Santinelli, C., 2021. DOM biological lability in an estuarine system in two contrasting periods. J. Mar. Sci. Eng. 9, 1–13. https://doi.org/10.3390/jmse9020172.

Roshan, S., DeVries, T., 2017. Efficient dissolved organic carbon production and export in the oligotrophic ocean. Nat. Commun. 8, 2036. https://doi.org/10.1038/s41467-017-02227-3.

Santinelli, C., 2015. DOC in the Mediterranean Sea. Biogeochemistry of Marine Dissolved Organic Matter, Second edition, pp. 579–608.

Santinelli, C., Follett, C., Retelletti Brogi, S., Xu, L., Repeta, D., 2015. Carbon isotope measurements reveal unexpected cycling of dissolved organic matter in the deep Mediterranean Sea. Mar. Chem. 177, 267–277. https://doi.org/10.1016/j.marchem.2015.06.018.

Santos, M., Oliveira, H., Pereira, J.L., Pereira, M.J., Gonçalves, F.J.M., Vidal, T., 2019. Flow cytometry analysis of low/high DNA content (LNA/HNA) bacteria as bioindicator of water quality evaluation. Ecol. Indic. 103, 774–781. https://doi.org/10.1016/j.ecolind.2019.03.033.

Shukla, T., Sen, I.S., Boral, S., Sharma, S., 2021. A time-series record during COVID-19 lockdown shows the high resilience of dissolved heavy metals in the Ganga River. Environ. Sci. Technol. Lett. 8, 301–306. https://doi.org/10.1021/acs.estlett.0c00982.

Stanley, E.H., Powers, S.M., Lottig, N.R., Buffam, I., Crawford, J.T., 2012. Contemporary changes in dissolved organic carbon (DOC) in human-dominated rivers: is there a role for DOC management? Freshw. Biol. 57, 26–42. https://doi.org/10.1111/j.1365-2427.2011.02613.x.

Stedmon, C.A., Nelson, N.B., 2015. The optical properties of DOM in the ocean. Biogeochemistry of Marine Dissolved Organic Matter, Second edition, pp. 481–508 https://doi.org/10.1016/B978-0-12-405940-5.00010-8.

Thrane, J.E., Hessen, D.O., Andersen, T., 2014. The absorption of light in lakes: negative impact of dissolved organic carbon on primary productivity. Ecosystems 17, 1040–1052.

Tobías, A., Carnerero, C., Reche, C., Massagué, J., Via, M., Minguillón, M.C., Alastuey, A., Querol, X., 2020. Changes in air quality during the lockdown in Barcelona (Spain) one month into the SARS-CoV-2 epidemic. Sci. Total Environ. 726, 138540. https://doi.org/10.1016/j.scitotenv.2020.138540.

UNWWAP (United Nations World Water Assessment Program), 2003. Water for people: water for life. UN World Water Development Report. UNESCO.

de Vicente, I., Ortega-Retuerta, E., Morales-Baquero, R., Reche, I., 2012. Contribution of dust inputs to dissolved organic carbon and water transparency in Mediterranean reservoirs. Biogeosciences 9, 5049–5060. https://doi.org/10.5194/bg-9-5049-2012.

Volpe, G., Colella, S., Brando, V.E., Forneris, V., La Padula, F., Di Cicco, A., Sammartino, M., Bracaglia, M., Artuso, F., Santoleri, R., 2019. Mediterranean Ocean colour level 3 operational multi-sensor processing. Ocean Sci. 15, 127–146. https://doi.org/10.5194/os-15-127-2019.

Wikner, J., Andersson, A., 2012. Increased freshwater discharge shifts the trophic balance in the coastal zone of the northern Baltic Sea. Glob. Chang. Biol. 18, 2509–2519. https://doi.org/10.1111/j.1365-2486.2012.02718.x.

Williams, P.J., Le, B., Ducklow, H.W., 2019. The microbial loop concept: a history, 1930–1974. J. Mar. Res. 77, 23–81. https://doi.org/10.1357/002224019828474359.

Xenopoulos, M.A., Barnes, R.T., Boodoo, K.S., Butman, D., Catalán, N., D'Amario, S.C., Fasching, C., Kothawala, D.N., Pisani, O., Solomon, C.T., Spencer, R.G.M., Williams, C.J., Wilson, H.F., 2021. How humans alter dissolved organic matter composition in freshwater: relevance for the earth's biogeochemistry. Biogeochemistry 154, 323–348. https://doi.org/10.1007/s10533-021-00753-3.

Zhang, X., Chen, Z., Shen, J., Zhao, S., Kang, J., Chu, W., Zhou, Y., Wang, B., 2020. Formation and interdependence of disinfection byproducts during chlorination of natural organic matter in a conventional drinking water treatment plant. Chemosphere 242, 125227. https://doi.org/10.1016/j.chemosphere.2019.125227.

Supplementary Material

Evidence of Covid-19 lockdown effects on riverine dissolved organic matter dynamics provides a proof-of-concept for needed regulations of anthropogenic emissions

Retelletti Brogi S.[1], Cossarini G. [2], Bachi G. [1], Balestra C.[2], Camatti E.[1,3], Casotti R.[4], Checcucci G. [1], Colella S.[5], Evangelista V. [1], Falcini F.[5], Francocci F.[6], Giorgino T.[7], Margiotta F. [4], Ribera d'Alcalà M. [4], Sprovieri M.[8], Vestri S. [1], Santinelli C. [1]

[1] *Istituto di Biofisica, CNR. Pisa, Italy.*

[2] *Istituto Nazionale di Oceanografia e Geofisica Sperimentale. Sgonico (TS), Italy.*

[3] *Istituto di Scienze Marine, CNR. Venezia, Italy.*

[4] *Stazione Zoologica Anton Dohrn. Napoli, Italy.*

[5] *Istituto di Scienze Marine, CNR. Roma, Italy*

[6] *Istituto per lo studio degli impatti Antropici e Sostenibilità in ambiente marino, CNR. Roma, Italy.*

[7] *Istituto di Biofisica, CNR. Milano, Italy.*

[8] *Istituto per lo studio degli impatti Antropici e Sostenibilità in ambiente marino, CNR. Campobello di Mazara (TP), Italy.*

Figure S1. Results of the specsse test within drEEM showing the effect of the model when adding more components, expressed as the sum of squared error for each model. The plots show that the 6 component model is the one with the lower error in both excitation (upper panel) and emission (lower panel).

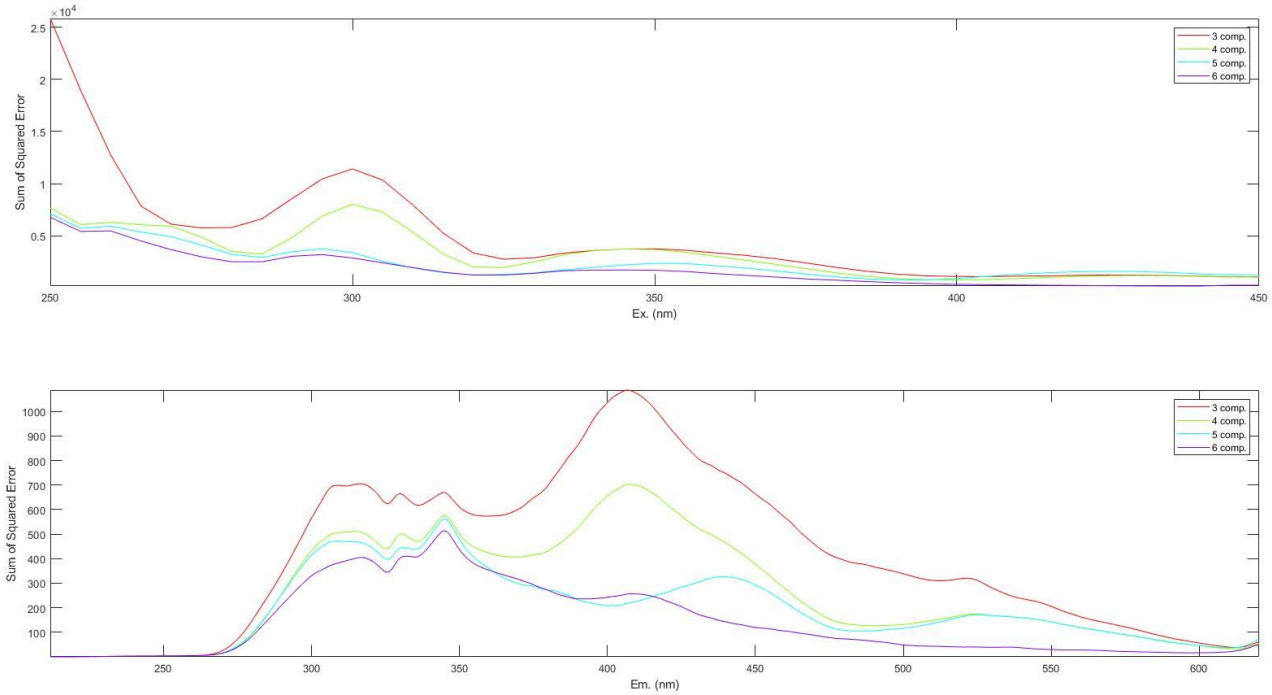

Figure S2. Example of inspection of the residuals for the validation of the PARAFAC model. Here we compare the 3 components model (upper panels) with the 6 components model (lower panels). The plots show the original sample on the left, the modeled one in the center, and the difference between the two on the right (i.e. the residuals)

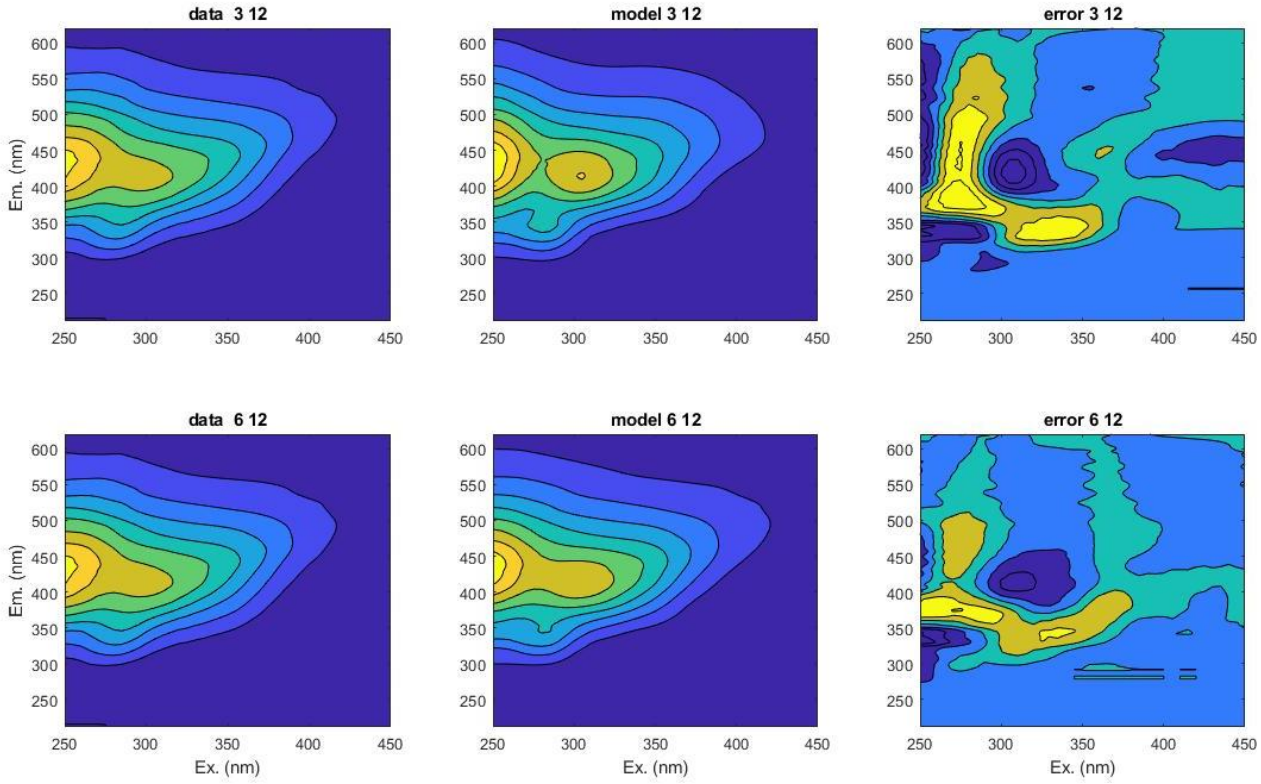

Figure S3. Core consistency results for the 6 components model.

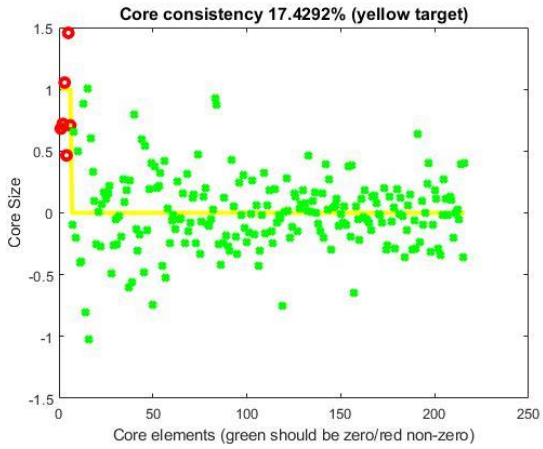

Figure S4. Results of the split validation tool within the drEEM

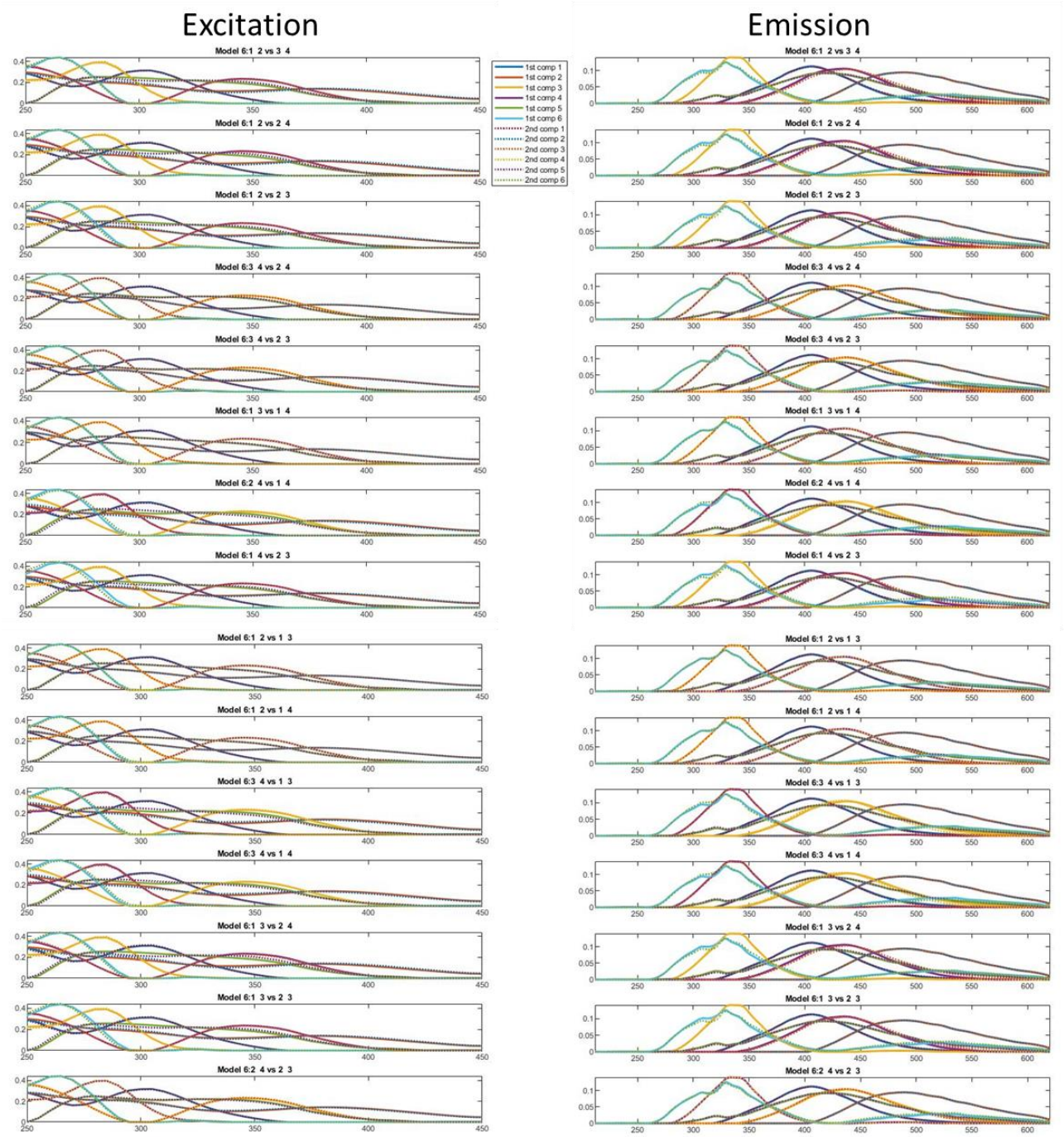

Figure S5. Results of the 6 components model validation carried out within the drEEM tool.

```
val6 =
  struct with fields:

                          Ex: [41×1 double]
                          Em: [500×1 double]
                           X: [468×500×41 double]
                IntensityUnit: 'RU'
                         nEx: 41
                         nEm: 500
                     nSample: 468
                          ID: {468×1 cell}
                   Xnotscaled: [468×500×41 double]
                   Preprocess: 'Normalised to unit variance in sample mode'
                        Split: [1×6 struct]
       Split_NumBeforeCombine: 4
                 Split_Style: 'alternating then combine'
        Split_NumAfterCombine: 6
           Split_Combinations: {'1  2'  '3  4'  '1  3'  '2  4'  '1  4'  '2  3'}
                Split_nSample: [234 234 234 234 234 234]
              Split_AnalRuns: [5 5 5 5 5 5]
     Split_PARAFAC_Initialise: 'Random'
        Split_PARAFAC_options: [1.0000e-06 2 0 0 0 0]
    Split_PARAFAC_constraints: [2 2 2]
      Split_PARAFAC_convgcrit: [1.0000e-06 1.0000e-06 1.0000e-06 1.0000e-06 1.0000e-06 1.0000e-06]
                      Model6: {3×1 cell}
               Val_ModelName: 'Model6'
              Val_Preprocess: 'Reversed normalisation to recover true scores'
                 Val_Source: 'Model6it_7'
                   Val_Err: 5.9662e+04
                    Val_It: 70
                  Val_Core: 17.4292
               Val_ConvgCrit: 1.0000e-06
             Val_Constraints: 'nonnegativity'
              Val_Initialise: 'random'
             Val_PercentExpl: 99.6152
                Val_CompSize: [48.0472 33.1062 30.8155 14.7680 21.0592 5.0615]
                 Val_Result: 'Overall Result= Validated for all comparisons'
             Val_Comparisons: {'AB vs CD,'  'AC vs BD,'  'AD vs BC,'}
         Val_Comparisons_Num: [3×2 double]
                Val_Matches: {4×1 cell}
                   Val_ExCC: {4×1 cell}
                   Val_EmCC: {4×1 cell}
                 Val_Splits: {'AB'  'CD'  'AC'  'BD'  'AD'  'BC'}
              Val_SplitsNum: [1 2 3 4 5 6]
```

Figure S6. Excitation (blue) and emission (red) spectra of the six components validated by the application of PARAFAC analysis to 533 EEMs (2020-2021 dataset plus the data from 2014-2015). The numbers indicate the wavelength of each spectrum peak.

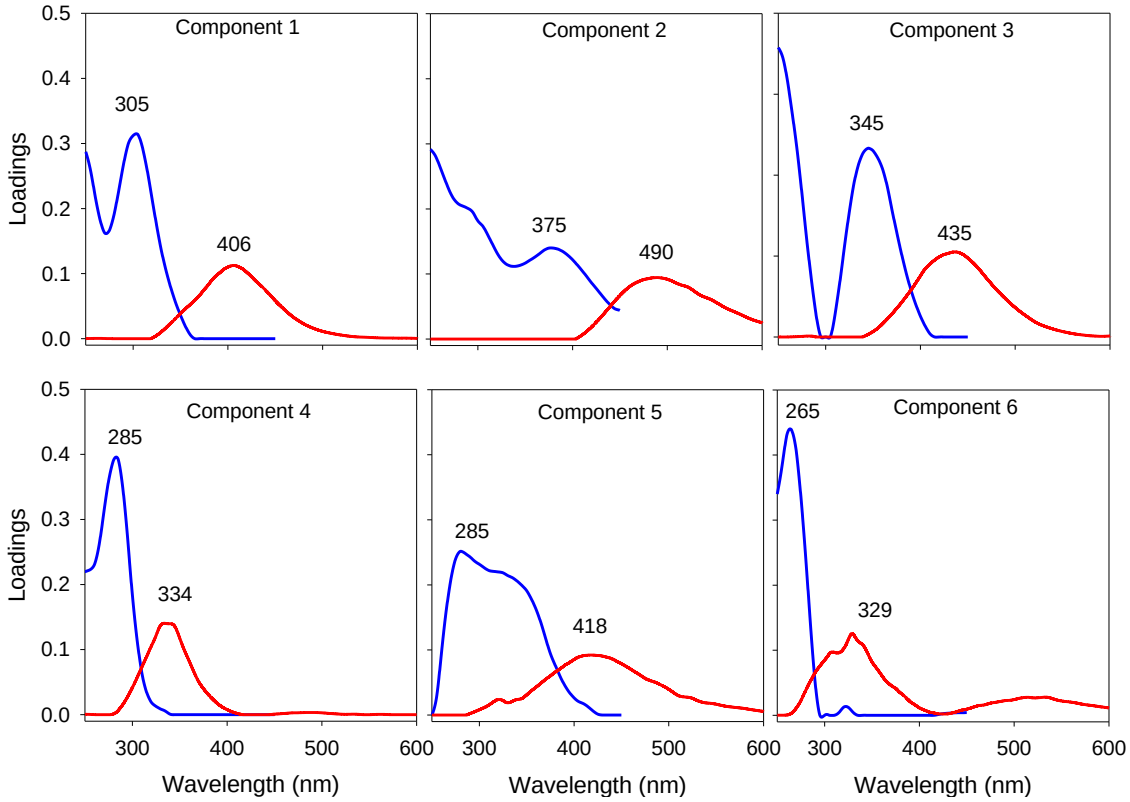

Figure S7. Contour plots of the components validated by PARAFAC.

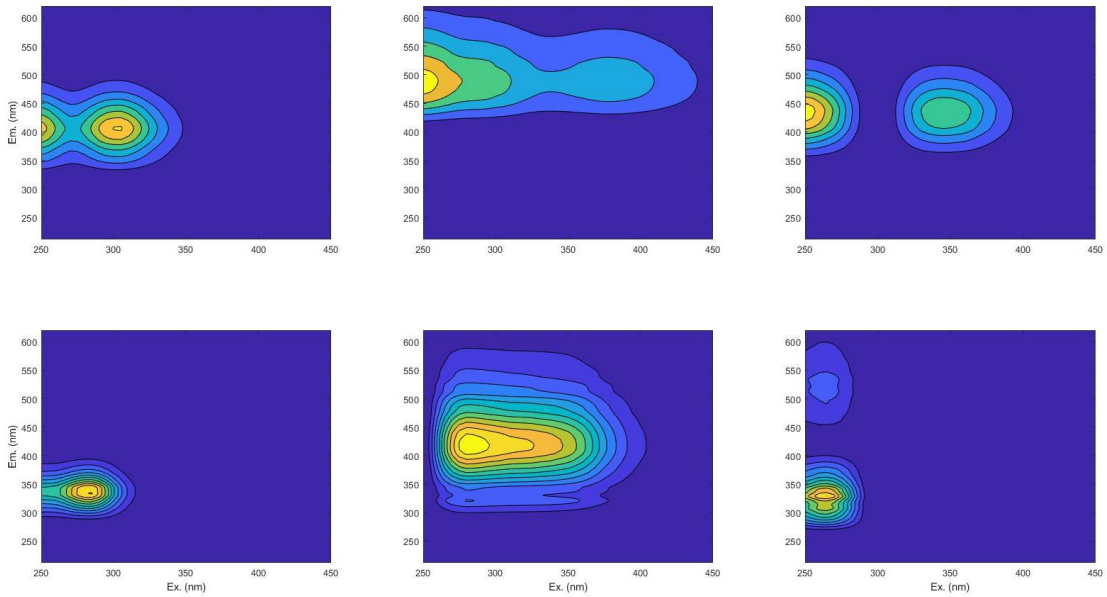

Table S1. Characteristics of the components, their characterization, and references to similar components found in the literature. The comparison with the components was done either by using the Openfluor database (Murphy et al., 2014b) or by comparing the excitation and emission maxima with published components not present in the database.

Components	λex peak (nm)	λem peak (nm)	Idetification	Similar components
C1	<250, 305	406	Microbial humic-like	**C1** Retelletti Brogi et al., 2020 **C5** Lapierre and Del Giorgio, 2014 **C2** Murphy et al., 2011 **C4** Meng et al., 2013 **C6** Maie et al., 2014 **C3** Lambert et al., 2016 **C1** Ferretto et al., 2017 **Peak β** Parlanti et al., 2000
C2	<250, 375	490	Terrestrial humic-like	**C2** Retelletti Brogi et al., 2020 **C2** Meng et al., 2013 **C1** Maie et al., 2014 **C2** Murphy et al., 2014a **C2** Lambert et al., 2016 **Peak α** Parlanti et al., 2000
C3	<250, 345	435	Fulvic-like	**C3** Retelletti Brogi et al., 2020 **C4** Lapierre and Del Giorgio, 2014 **C360/456** Stedmon et al., 2011 **C1** Maie et al., 2014 **C1** Lambert et al., 2016 **C3** Ferretto et al., 2017
C4	285	334	Protein-like	**C4** Retelletti Brogi et al., 2020 **C5** Murphy et al., 2006 **C3** Stedmon et al., 2011 **C3** Hur and Cho, 2012 **C3** Meng et al., 2013 **C5** Lambert et al., 2016 **C2** Ferretto et al., 2017 **Peak δ** Parlanti et al., 2000
C5	285	418	Fulvic-like	**C2** Chen et al., 2018 **C1** Lee et al., 2020 **C5** Stedmon and Markager, 2005 **C1** Yamashita et al., 2011 **C2** Murphy et al., 2006
C6	265	329	PAH-like	**C1** Gonnelli et al., 2016 **C3** Nie et al., 2016 **C6** Kothawala et al., 2014 **C3** Meng et al., 2013 **C7** Maie et al., 2014 **Peak δ** Parlanti et al., 2000

Chen, M., Jung, J., Lee, Y.K., Hur, J., 2018. Surface accumulation of low molecular weight dissolved organic matter in surface waters and horizontal off-shelf spreading of nutrients and humic-

like fluorescence in the Chukchi Sea of the Arctic Ocean. Sci. Total Environ. 639, 624–632. https://doi.org/10.1016/J.SCITOTENV.2018.05.205

Ferretto, N., Tedetti, M., Guigue, C., Mounier, S., Raimbault, P., Goutx, M., 2017. Spatio-temporal variability of fluorescent dissolved organic matter in the Rhône River delta and the Fos-Marseille marine area (NW Mediterranean Sea, France). Environ. Sci. Pollut. Res. 24, 4973–4989. https://doi.org/10.1007/s11356-016-8255-z

Gonnelli, M., Galletti, Y., Marchetti, E., Mercadante, L., Retelletti Brogi, S., Ribotti, A., Sorgente, R., Vestri, S., Santinelli, C., 2016. Dissolved organic matter dynamics in surface waters affected by oil spill pollution: Results from the Serious Game exercise. Deep. Res. Part II Top. Stud. Oceanogr. 133, 88–99. https://doi.org/10.1016/j.dsr2.2016.05.027

Hur, J., Cho, J., 2012. Prediction of BOD, COD, and total nitrogen concentrations in a typical urban river using a fluorescence excitation-emission matrix with PARAFAC and UV absorption indices. Sensors 12, 972–986. https://doi.org/10.3390/s120100972

Kothawala, D.N., Stedmon, C.A., Müller, R.A., Weyhenmeyer, G.A., Köhler, S.J., Tranvik, L.J., 2014. Controls of dissolved organic matter quality: Evidence from a large-scale boreal lake survey. Glob. Chang. Biol. 20, 1101–1114. https://doi.org/10.1111/gcb.12488

Lambert, T., Teodoru, C.R., Nyoni, F.C., Bouillon, S., Darchambeau, F.F., Massicotte, P., Borges, A. V., 2016. Along-stream transport and transformation of dissolved organic matter in a large tropical river. Biogeosciences 13, 2727–2741. https://doi.org/10.5194/bg-13-2727-2016

Lapierre, J.F., Del Giorgio, P.A., 2014. Partial coupling and differential regulation of biologically and photochemically labile dissolved organic carbon across boreal aquatic networks. Biogeosciences 11, 5969–5985. https://doi.org/10.5194/bg-11-5969-2014

Lee, S.-A., Kim, T.-H., Kim, G., 2020. Tracing terrestrial versus marine sources of dissolved organic carbon in a coastal bay using stable carbon isotopes. Biogeosciences 17, 135–144. https://doi.org/10.5194/bg-17-135-2020

Maie, N., Sekiguchi, S., Watanabe, A., Tsutsuki, K., Yamashita, Y., Melling, L., Cawley, K.M., Shima, E., Jaffé, R., 2014. Dissolved organic matter dynamics in the oligo/meso-haline zone of wetland-influenced coastal rivers. J. Sea Res. 91, 58–69. https://doi.org/10.1016/j.seares.2014.02.016

Meng, F., Huang, G., Yang, X., Li, Z., Li, J., Cao, J., Wang, Z., Sun, L., 2013. Identifying the sources and fate of anthropogenically impacted dissolved organic matter (DOM) in urbanized rivers. Water Res. 47, 5027–5039. https://doi.org/10.1016/j.watres.2013.05.043

Murphy, K.R., Bro, R., Stedmon, C.A., 2014a. Chemometric Analysis of Organic Matter Fluorescence, in: Aquatic Organic Matter Fluorescence. pp. 339–375.

Murphy, K.R., Hambly, A., Singh, S., Henderson, R.K., Baker, A., Stuetz, R., Khan, S.J., 2011. Organic matter fluorescence in municipal water recycling schemes: Toward a unified PARAFAC model. Environ. Sci. Technol. 45, 2909–16. https://doi.org/10.1021/es103015e

Murphy, K.R., Ruiz, G.M., Dunsmuir, W.T.M., Waite, T.D., 2006. Optimized parameters for fluorescence-based verification of ballast water exchange by ships. Environ. Sci. Technol. 40, 2357–2362. https://doi.org/10.1021/es0519381

Murphy, K.R., Stedmon, C.A., Wenig, P., Bro, R., 2014b. OpenFluor- an online spectral library of auto-fluorescence by organic compounds in the environment. Anal. Methods 6, 658–661. https://doi.org/10.1039/C3AY41935E

Nie, Z., Wu, X., Huang, H., Fang, X., Xu, C., Wu, J., Liang, X., Shi, J., 2016. Tracking fluorescent dissolved organic matter in multistage rivers using EEM-PARAFAC analysis: implications of the secondary tributary remediation for watershed management. Environ. Sci. Pollut. Res. 23, 8756–8769. https://doi.org/10.1007/s11356-016-6110-x

Parlanti, E., Worz, K., Geoffroy, L., Lamotte, M., Wörz, K., Geoffroy, L., Lamotte, M., 2000. Dissolved organic matter Fluorescence spectroscopy as a tool to estimate biological activity in a coastal zone submitted to anthropogenic inputs. Org. Geochem. 31, 1765–1781. https://doi.org/0146-6380/00/$

Retelletti Brogi, S., Balestra, C., Casotti, R., Cossarini, G., Galletti, Y., Gonnelli, M., Vestri, S., Santinelli, C., 2020. Time resolved data unveils the complex DOM dynamics in a Mediterranean river. Sci. Total Environ. https://doi.org/10.1016/j.scitotenv.2020.139212

Stedmon, C. a., Markager, S., 2005. Resolving the variability of dissolved organic matter fluorescence in a temperate estuary and its catchment using PARAFAC analysis. Limnol. Oceanogr. 50, 686–697. https://doi.org/10.4319/lo.2005.50.2.0686

Stedmon, C.A., Amon, R.M.W., Rinehart, A.J., Walker, S.A., 2011. The supply and characteristics of colored dissolved organic matter (CDOM) in the Arctic Ocean: Pan Arctic trends and differences. Mar. Chem. 124, 108–118. https://doi.org/10.1016/j.marchem.2010.12.007

Yamashita, Y., Kloeppel, B.D., Knoepp, J., Zausen, G.L., Jaffé, R., 2011. Effects of Watershed History on Dissolved Organic Matter Characteristics in Headwater Streams. Ecosystems. https://doi.org/10.1007/s10021-011-9469-z

Figure S8. (a) Total industrial activity in Tuscany from January 2005 to September 2020, the dashed line represents the average between 2005 and 2019, the standard deviation is indicated by the continuous lines. The inset shows a zoom of 2020 (January to September). (b) Tourist arrivals in Tuscany from 2012 to 2020. (c) Total movements (in or out) in the two major airports in Tuscany from 2014 to 2020 (data from 2019 were not available). (d) Land transportation movements between March and December 2020, from the Google community mobility report (categorized by movement purpose).

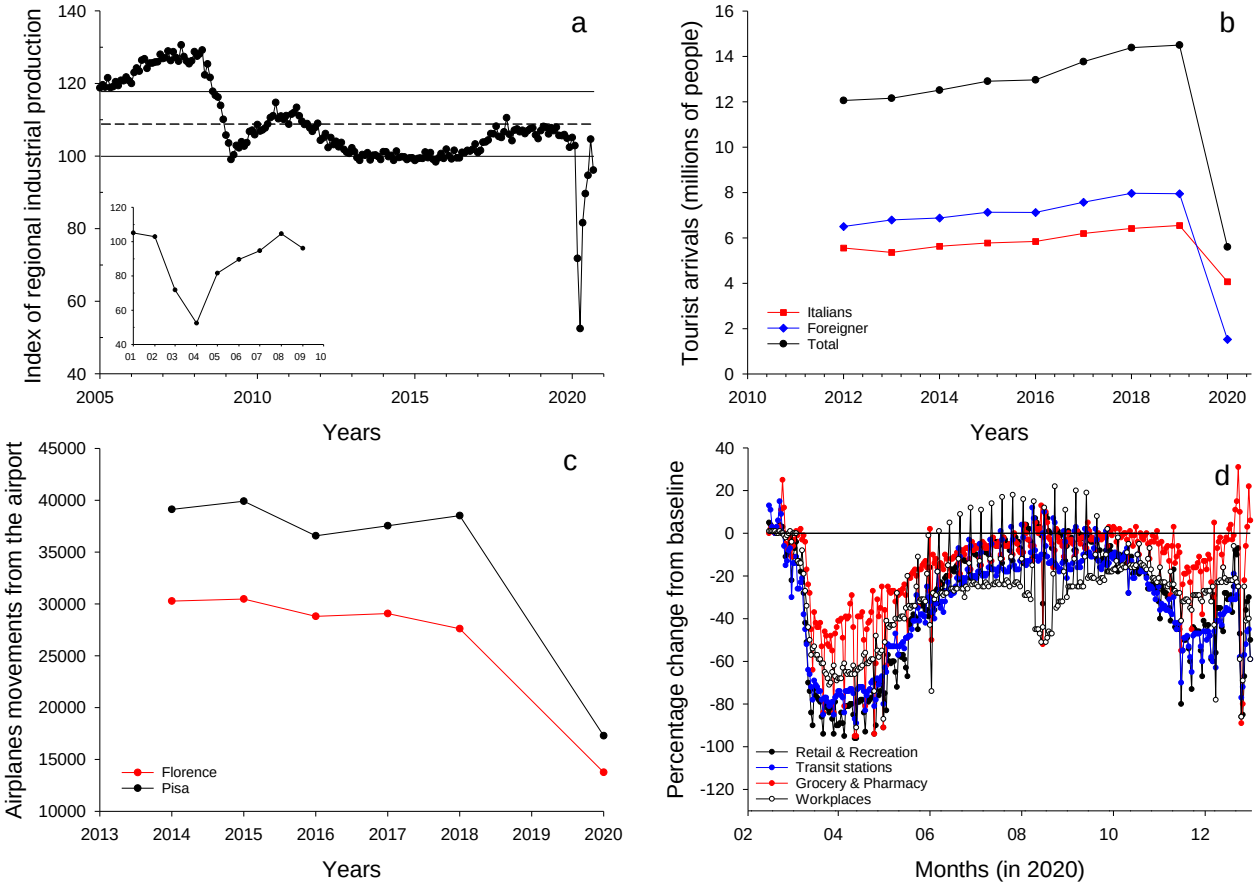

Table S2. Results of the stepwise regression. The sequence of inclusion (first column) of the variables (second column) in the regression model based on the marginal p-level (third column). Values of the coefficients and their standard error for the included variables (fourth and fifth column). Root Mean Square Error (RMSE) of the reconstructed DOC time series by the partial and final regression models (sixth column).

Steps	**Variables**	**min-max of the variable**	**p-values**	**coefficient of the model**	**Standard Error of the coefficient**	**RMSE of the model [μM]**
	Constant [μM]			239.8		
1	Runoff-90d *[m^3/s]*	0-400	$4.73 \cdot 10^{-09}$	-0.387	0.062	60.8
2	Lockdown period Mar-Jul 2020 [-]	0-1	$6.08 \cdot 10^{-22}$	-126.4	10.9	55.2
3	Temperature [°C]	5-32	$7.63 \cdot 10^{-16}$	7.268	0.795	45.5
4	Runoff-2d *[m^3/s]*	0-1000	$3.10 \cdot 10^{-07}$	0.160	0.030	42.9
5	Lockdown period Aug-Nov 2020 [-]	0-1	$3.12 \cdot 10^{-04}$	-34.5	9.3	40.8
6	Runoff-30d *[m^3/s]*	0-600	$8.80 \cdot 10^{-03}$	-0.176	0.066	39.7
7	HPA *[cells/ml]*	0-1E7	$2.57 \cdot 10^{-03}$	$-6.7 \cdot 10^{-06}$	$2.2 \cdot 10^{-06}$	38.8
Not included in the model	runoff-1d [m3/s]	0-1000	$3.29 \cdot 10^{-01}$			
	Lockdown period Mar-May 2020 [-]	0-1	1.00			
	Lockdown period Mar-June 2020 [-]	0-1	$3.48 \cdot 10^{-01}$			
	Lockdown period Mar-Aug 2020 [-]	0-1	$4.87 \cdot 10^{-01}$			
	Lockdown period Jul-Oct 2020 [-]	0-1	$5.05 \cdot 10^{-01}$			
	Lockdown period Jul-Dec 2020 [-]	0-1	$2.79 \cdot 10^{-01}$			
	Lockdown period Jul2020-Jan2021 [-]	0-1	$3.59 \cdot 10^{-01}$			
	Lockdown period Jun-Oct 2020 [-]	0-1	$5.05 \cdot 10^{-01}$			
	Lockdown period Jul-Nov2020 [-]	0-1	$8.40 \cdot 10^{-01}$			
	Lockdown period May-Nov 2020 [-]	0-1	$2.59 \cdot 10^{-01}$			
	runoff-3d [m3/s]	0-1000	$8.36 \cdot 10^{-01}$			
	runoff-60d [m3/s]	0-300	$5.44 \cdot 10^{-01}$			
	runoff-120d [m3/s]	0-200	$5.44 \cdot 10^{-01}$			

Figure S9. Arno River absorption coefficient at 254 nm (a_{254}) in 2014, 2015, 2020, and 2021, error bars represent the standard deviation (n=3).

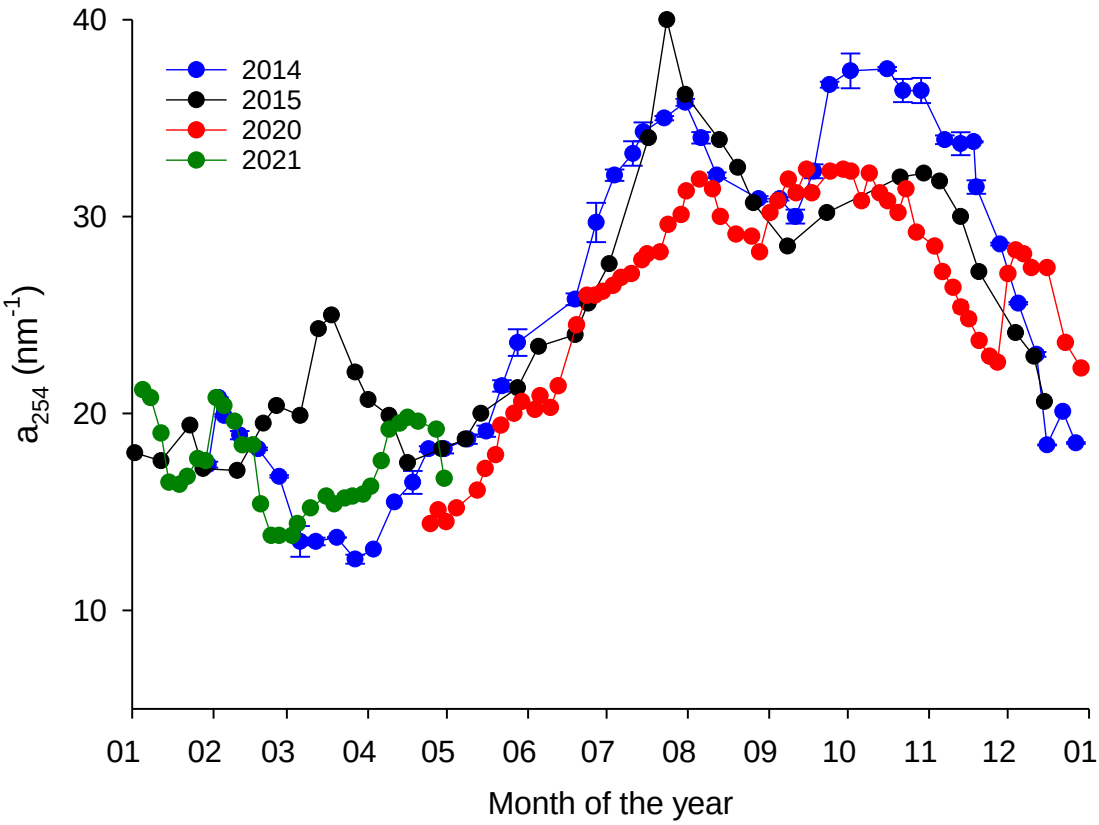

Figure S10. Annual trend of the 6 components identified by PARAFAC analysis of the EEMs in 2014, 2015, 2020, and 2021, error bars represent the standard deviation (n=3).

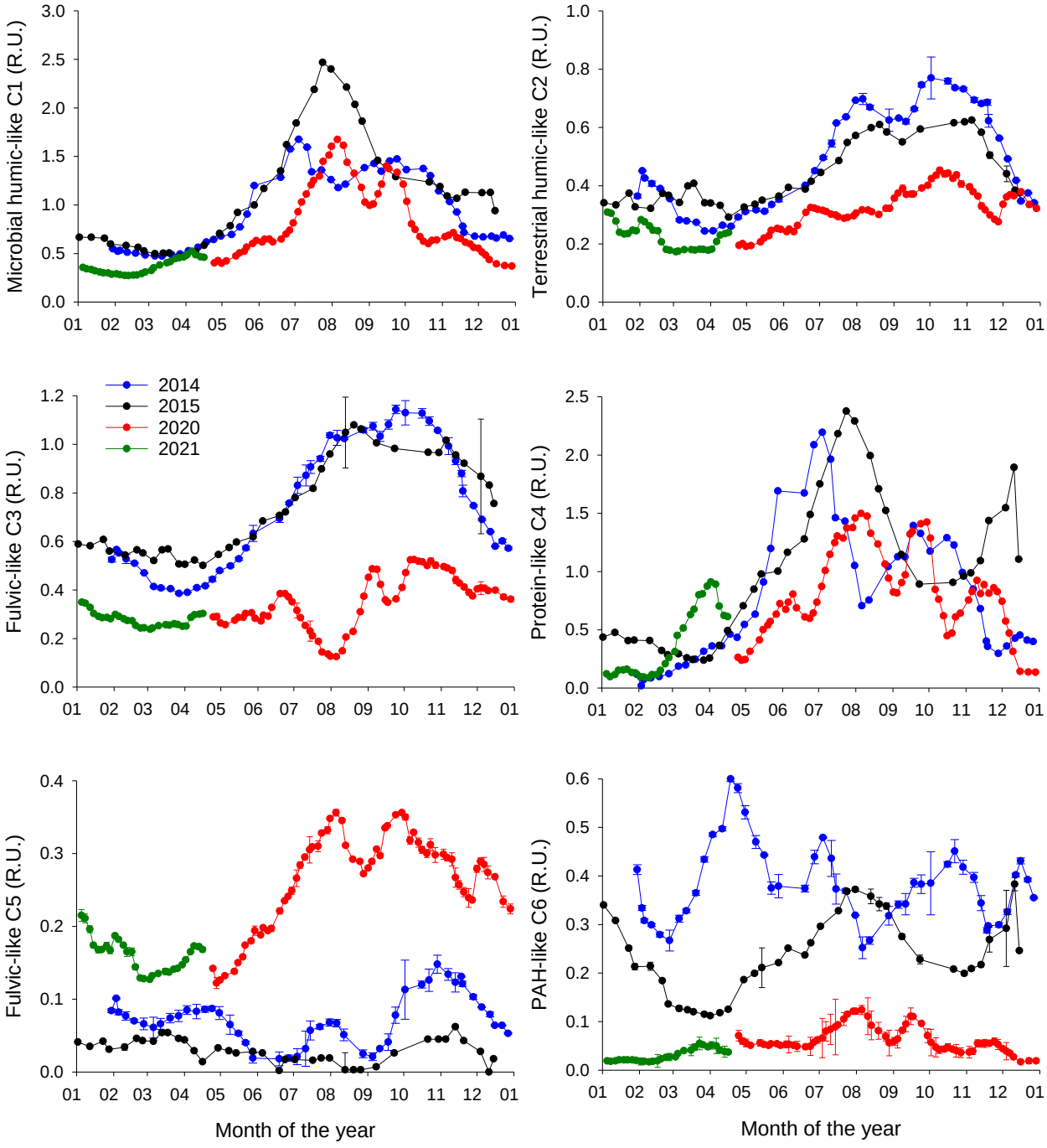

Figure S11. Annual trend of high nucleic acid heterotrophic prokaryotes (HP), shown as a percentage of the total HP.

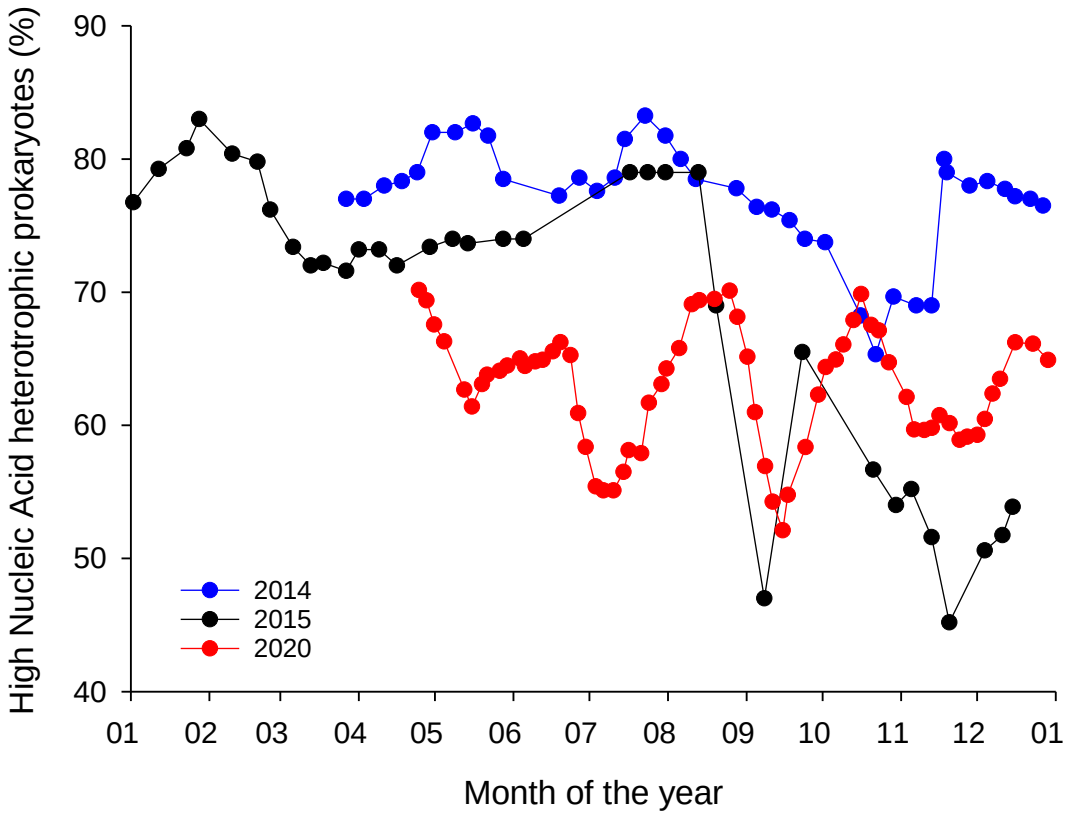

Figure S12. Distribution of dissolved organic carbon (DOC) in the coastal area in front of the Arno River estuary on May 5th, 2020.

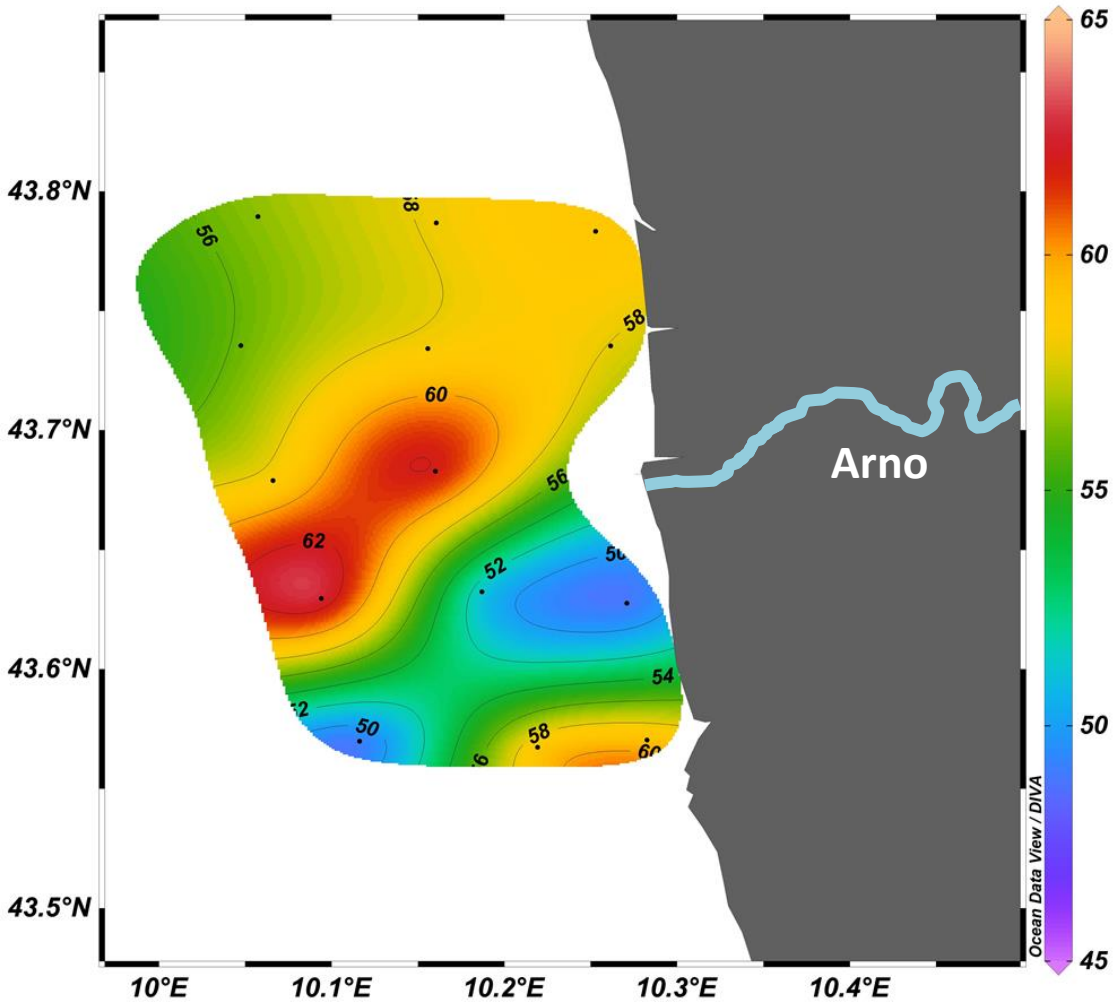

Figure S13. Comparison of monthly means of air temperature (a), precipitation (b), and discharge (c) between 2020 (dark line) and the climatology (colored lines and shaded areas). Light-colored areas represent the 05th and 95th percentile, dark-colored areas represent the 25th and 75th percentile.

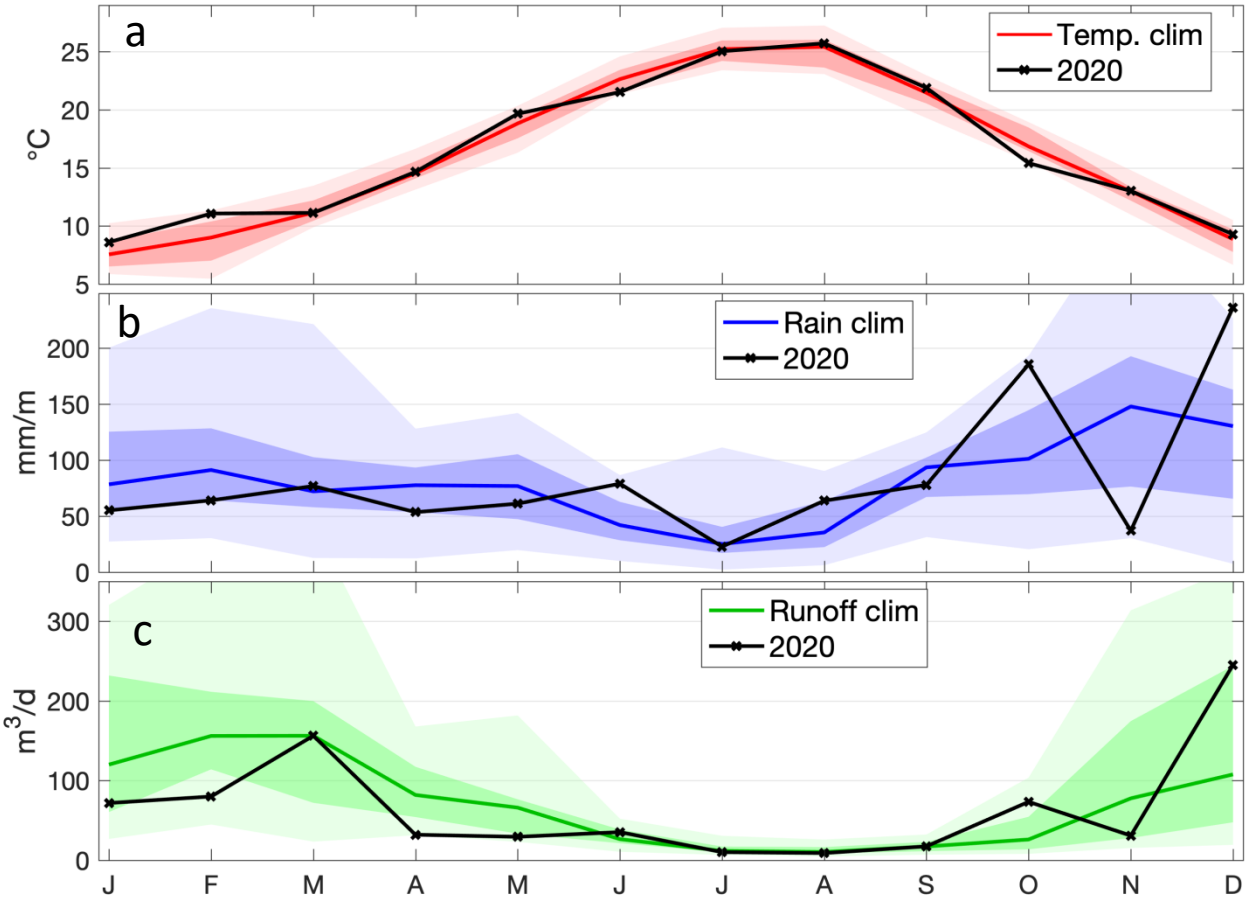

Figure S14. River surface water temperature in 2014, 2015, 2020 and 2021